

# Bootstrap and the physical values of $\pi N$ resonance parameters.

K. Semenov-Tian-Shansky,<sup>\*</sup> Alexander V. Vereshagin,<sup>†</sup> and Vladimir V. Vereshagin<sup>‡</sup>

*St.-Petersburg State University, St.Petersburg, Petrodvoretz, 198504, Russia*

## Abstract

This is the 6th paper in the series developing the formalism to manage the effective scattering theory of strong interactions. Relying on the theoretical scheme suggested in our previous publications we concentrate here on the practical aspect and apply our technique to the elastic pion-nucleon scattering amplitude. We test numerically the  $\pi N$  spectrum sum rules that follow from the tree level bootstrap constraints. We show how these constraints can be used to estimate the tensor and vector  $NN\rho$  coupling constants. At last, we demonstrate that the tree-level low energy expansion coefficients computed in the framework of our approach show nice agreement with known experimental data. These results allow us to claim that the extended perturbation scheme is quite reasonable from the computational point of view.

PACS numbers: 02.30.Lt, 11.15.Bt, 13.75.Gx, 14.20.Gk

---

<sup>\*</sup>Electronic address: cyr'stsh@mail.ru; Also at Institut für Theoretische Physik II, Ruhr-Universität Bochum, D-44780 Bochum, Germany

<sup>†</sup>Electronic address: Alexander.Vereshagin@ift.uib.no; Also at University of Bergen, Institute of Physics and Technology, Allegt.55, N5007 Bergen, Norway

<sup>‡</sup>Electronic address: vvv@AV2467.spb.edu

## I. INTRODUCTION

In our previous publications (see [1, 2]) we developed the generic construction of efficient perturbation scheme intended for effective scattering theories of strong interaction<sup>1</sup>. This study is still in progress. Meanwhile, already our present results appear to be quite sufficient to justify the usage of experimental data for checking the correctness of *tree level* bootstrap constraints for the effective theory parameters.

Due to the renormalization invariance of bootstrap constraints (see [2]) those constraints of arbitrary loop level present exact (self-consistency type) numerical limitations for the admissible values of renormalization prescriptions. These prescriptions are the only fundamental observables of a theory and, hence, every kind of theoretical constraints for their values can be directly compared with experimental data. This is true irrelatively to the loop order of the bootstrap constraints under consideration. For this reason it seems us natural to perform the numerical testing of the tree level bootstrap constraints using the available experimental data. This will allow us to check the physical reasonability of our main postulates and, at the same time, to demonstrate the practical output of the formalism discussed in the above-cited articles.

This paper is designed as a regular introduction to the corresponding calculational methods. We demonstrate the details of calculational procedure beginning with general formulae and ending with numerical results.

As an example we consider below the elastic pion-nucleon scattering process. We derive and compare with known data several sum rules for the parameters (coupling constants and masses) of pion-nucleon resonances that follow from the tree level bootstrap constraints.

Besides, we show that the latter constraints provide reasonable estimates for the numerical values of experimentally known (see, e.g., [8]) phenomenological constants  $G_T$  and  $G_V$  which describe the tensor and vector types of  $\rho$ -meson coupling to nucleon.

Finally, we present the results for tree level values of low energy expansion coefficients of pion-nucleon scattering amplitude around the cross-symmetric point  $(t, \nu_t) = (0, 0)$ . The values of these coefficients are, by no doubt, affected by loop corrections. Nevertheless, as follows from our estimates, the tree level values obtained in the framework of extended

---

<sup>1</sup> Preliminary analysis has been published in [3] - [7].

perturbation scheme turn out to be very close to the experimental ones. This fact suggests that the extended perturbation scheme is quite reasonable from the physical point of view.

## II. PRELIMINARIES

In this Section we quote those results of the papers [1, 2] which constitute the theoretical background of our calculations below. It is implied that the reader is familiar with the notions and terminology introduced in those articles.

First of all let us remind that we only consider a special class of effective theories called in [2] as *localizable*. To assign meaning to individual terms of Dyson series for such a theory we switch to the so-called *extended perturbation scheme* which contains supplementary resonance fields. This procedure can be treated as a special kind of summation of an infinite set of graphs (with the same number of loops) that appear in every order of the initial Dyson series.

The extended perturbation scheme is just an auxiliary construction which allows us to define rigorously the perturbation expansion in the case of infinite component effective theory. In particular, the  $S$ -matrix calculated in the framework of extended perturbation scheme still acts on the space of asymptotic states that correspond to true stable (with respect to strong decays) particles. The supplementary resonance fields do not correspond to any asymptotic states and hence may appear only in the inner lines of graphs which describe the scattering processes of stable particles. In this paper we consider the case when there are only two species of stable particles, namely, pions and nucleons.

The list of the results of [1, 2] which we rely upon in this paper reads:

- In the framework of effective theory an arbitrary renormalized  $S$ -matrix graph can be presented in the form solely constructed from the minimal propagators and resultant vertices of various levels. The true loop order of a given graph is just a number of explicitly drawn loops plus the sum of level indices of its vertices.
- All the information needed to completely fix the kinematical structure of renormalized  $S$ -matrix elements of a given loop order  $L$  is contained in the numerical values of resultant parameters of  $L$ th and lower levels.
- By construction, the resultant parametrization implies using the scheme of *renormal-*

*ized perturbation theory.* This means that the relevant resultant parameters (in the case we analyze below — the 0th level ones) should be considered as fundamental physical observables of the theory.

These results are based on *summability* and *uniformity* requirements which are the corner stones of our extended perturbation scheme. The motivation for accepting these two requirements is presented in [2].

The uniformity requirement is formulated as follows: *the degree of the bounding polynomial which specifies the asymptotics of a given loop order amplitude must be the same as that specifying the asymptotics of the full (non-perturbative) amplitude of the process under consideration.*

The summability requirement reads: *in every sufficiently small domain of the complex space of kinematical variables there must exist an appropriate order of summation of the formal series of contributions coming from the graphs with given number of loops, such that the reorganized series converges. Altogether, these series must define a unique analytic function with only those singularities that are presented in the contributions of individual graphs.*

As a system of domains in which we require the  $2 \rightarrow 2$  amplitude to be summable we choose three hyperlayers

$$B_x \{x \in \mathbb{R}, \nu_x \in \mathbb{C}; x \sim 0\}, \quad (x = s, t, u).$$

Here  $s, t, u$  stand for conventional Mandelstam variables; the energy-like variables  $\nu_x$  are defined as follows:

$$\nu_s \equiv (u - t); \quad \nu_t \equiv (s - u); \quad \nu_u \equiv (t - s). \quad (1)$$

We imply that the full amplitudes under consideration satisfy Regge asymptotic conditions, at least, at sufficiently small values of the momentum transfer. With respect to tree level  $2 \rightarrow 2$  amplitudes this means that they are described by the polynomially bounded meromorphic functions of pair energies (at fixed value of the corresponding momentum transfer). The bounding polynomial degree in every hyperlayer  $B_x$  is fixed by the value of the relevant Regge intercept.

The results of [2] define the sequence of steps one should follow to derive the tree level bootstrap constraints for  $2 \rightarrow 2$  scattering amplitude:

1. Consider the general structure of the amplitude and single out the invariant formfactors.
2. Draw all loopless graphs for the amplitude of the process under consideration using Feynman rules of the extended perturbation scheme.
3. Classify the possible types of triple vertices in accordance with quantum numbers of the line corresponding to a virtual particle.
4. Construct the analytic expressions for individual graph contributions only using the minimal propagators and resultant vertices.
5. Perform a *formal* summation over all possible kinds of vertices and internal lines. This will result in the formal infinite sum of pole terms coming from the resonance exchange graphs plus a formal power series in two independent variables stemming from the pointlike vertices.
6. Now, being guided by summability and uniformity principles and applying the technique of Cauchy forms, convert a disordered sum of amplitude graphs into a rigourously defined expressions in three hyperlayers  $B_x$  ( $x = s, t, u$ ). The principle parts of the corresponding Cauchy forms are determined by the individual resonance exchange contributions. The bounding polynomial degrees are dictated by the values of corresponding Regge intercepts.
7. In three intersection domains

$$D_s = B_t \cap B_u, \quad D_t = B_u \cap B_s, \quad D_u = B_s \cap B_t$$

require the equality of different Cauchy forms presenting the same invariant amplitude in different hyperlayers  $B_x$  ( $x = s, t, u$ ). This will result in appearing of an infinite system of bootstrap conditions constraining the allowed values of fundamental observables of a theory (triple coupling constants and mass parameters). Besides, this system will also completely determine the allowed form of the 4-leg pointlike vertex.

8. Finally, choose those bootstrap constraints which can be compared with presently known data and perform the numerical testing.

Below we literally follow this step-by-step instruction and show all the details of corresponding calculations. This will allow us to omit these details in subsequent publications devoted to the analysis of more sophisticated cases.

In this paper we consider a concrete process and employ experimental data. Thus it is natural to take account of certain well established phenomenology already on the stage of constructing the amplitude. For this reason we take the isotopic invariance as an exact symmetry of strong interaction. Such restrictions are kept automatically when one uses experimental data to verify theoretical results. On the other hand, they do not affect the mathematical scheme developed in [2] and can easily be relaxed if necessary. Note that we suggest the absence of massless hadrons with spin  $J \geq 1$  which our technique cannot handle so far. This suggestion is also supported by experiment.

### III. STRUCTURE OF THE AMPLITUDE AND RESULTANT VERTICES

The amplitude  $M_{a\alpha}^{b\beta}$  of the reaction

$$\pi_a(k) + N_\alpha(p, \lambda) \rightarrow \pi_b(k') + N_\beta(p', \lambda')$$

can be presented in the following form:

$$M_{a\alpha}^{b\beta} = \left\{ \delta_{ba} \delta_{\beta\alpha} M^+ + i \varepsilon_{bac} (\sigma_c)_{\beta\alpha} M^- \right\}. \quad (2)$$

Here

$$M^\pm = \bar{u}(p', \lambda') \left\{ A^\pm + \left( \frac{\not{k} + \not{k}'}{2} \right) B^\pm \right\} u(p, \lambda), \quad (3)$$

$a, b, c = 1, 2, 3$  and  $\alpha, \beta = 1, 2$  stand for the isospin indices,  $\lambda, \lambda'$  — for polarizations of the initial and final nucleons, respectively,  $\bar{u}(p', \lambda')$ ,  $u(p, \lambda)$  — for Dirac spinors,  $\sigma_c$  — for Pauli matrices:

$$[\sigma_a, \sigma_b]_- = 2i \varepsilon_{abc} \sigma_c,$$

and  $\not{p} \equiv p_\mu \gamma^\mu$ . The invariant amplitudes  $A^\pm$  and  $B^\pm$  are considered depending on arbitrary pair of Mandelstam variables

$$s \equiv (p + k)^2, \quad t \equiv (k - k')^2, \quad u \equiv (p - k')^2.$$

To compute the tree level expressions for  $A^\pm$  and  $B^\pm$  one needs to collect contributions from the graphs shown in Fig. 1.

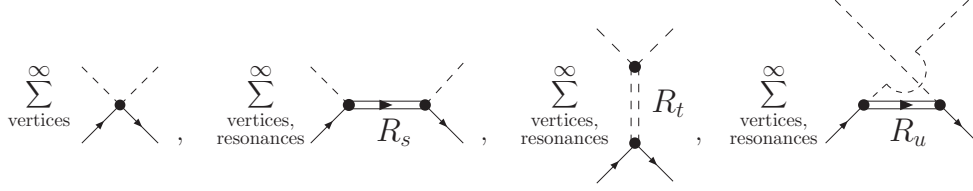


FIG. 1: Tree level graphs.  $R_s$ ,  $R_t$  and  $R_u$  stand for all admissible resonances in  $s$ -,  $t$ -, and  $u$ -channels, respectively; the formal summation over all possible kinds of vertices and internal lines is implied.

For this one needs to specify the form of minimal propagators and resultant triple vertices of three kinds: pion-pion-meson ( $\pi\pi M$ ), antinucleon-nucleon-meson ( $\bar{N}NM$ ) and pion-nucleon-baryon ( $\pi NB$ ). There is no need in explicit parametrization of the resultant point-like vertex  $N\bar{N}\pi\pi$  because, as shown in [2], its contribution turns out to be entirely fixed by the first kind bootstrap conditions.

The inner lines of graphs in Fig. 1 may correspond to mesons (dashed) and baryons (solid). There are two families of meson resonances which can give a contribution. The first one contains those with isospin  $I = 0$ , even spin  $J = 0, 2, \dots$  and positive parity  $P = +1$ . We denote the corresponding fields <sup>2</sup> as  $S_{\mu_1 \dots \mu_J}$ . The second meson family contains isovector resonances ( $I = 1$ ) with odd spin values  $J = 1, 3, \dots$  and negative parity  $P = -1$ ; their fields we denote as  $V_{\mu_1 \dots \mu_J}^a$  ( $a = 1, 2, 3$ ) (when forming scalar and vector products we omit the isospin indices and write isotopic vectors in boldface).

It is convenient to classify possible baryon resonances according to their *normality*  $\mathcal{N}$ :

$$\mathcal{N} \equiv (-1)^{(J-1/2)} P.$$

Here spin  $J = l + 1/2$  ( $l = 0, 1, \dots$ ). Therefore, only four families of baryon resonances contribute to the amplitude under consideration. We denote them as follows ( $\alpha = 1, 2$  and  $a = 1, 2, 3$  stand for the isotopic indices; spinor indices are omitted):

$$(I = 1/2, \mathcal{N} = +1) \implies R_{\mu_1 \dots \mu_l}^\alpha;$$

$$(I = 3/2, \mathcal{N} = +1) \implies \Delta_{\mu_1 \dots \mu_l}^{a\alpha};$$

$$(I = 1/2, \mathcal{N} = -1) \implies \hat{R}_{\mu_1 \dots \mu_l}^\alpha;$$

$$(I = 3/2, \mathcal{N} = -1) \implies \hat{\Delta}_{\mu_1 \dots \mu_l}^{a\alpha}.$$

<sup>2</sup> We use the Rarita-Schwinger formalism [9].

For example, the famous  $\Delta(1232)$  resonance ( $I, J = 3/2, P = +1$ ) has negative normality; in our notations it belongs to the family  $\widehat{\Delta}$ . Also, it should be kept in mind that the lightest particle with  $l = 0$  (spin  $J = 1/2$ ) in the family  $R$  is just a nucleon.

The resultant vertices are defined and can be properly written down in momentum space only [2]. However, the 3-leg resultant vertices provide an exception; they can be read from the following Hamiltonian monomials (we use  $\gamma_5 = -i\gamma^0\gamma^1\gamma^2\gamma^3$ ):

$$H(\pi NR) = ig_R \overline{N} \boldsymbol{\sigma} \gamma_5 R_{\mu_1 \dots \mu_l} \partial^{\mu_1} \dots \partial^{\mu_l} \boldsymbol{\pi} + H.c.; \quad (4)$$

$$H(\pi N \widehat{R}) = g_{\widehat{R}} \overline{N} \boldsymbol{\sigma} \widehat{R}_{\mu_1 \dots \mu_l} \partial^{\mu_1} \dots \partial^{\mu_l} \boldsymbol{\pi} + H.c.; \quad (5)$$

$$H(\pi N \Delta) = ig_{\Delta} \overline{N} \gamma_5 P_{3/2} \boldsymbol{\Delta}_{\mu_1 \dots \mu_l} \partial^{\mu_1} \dots \partial^{\mu_l} \boldsymbol{\pi} + H.c.; \quad (6)$$

$$H(\pi N \widehat{\Delta}) = g_{\widehat{\Delta}} \overline{N} P_{3/2} \widehat{\boldsymbol{\Delta}}_{\mu_1 \dots \mu_l} \partial^{\mu_1} \dots \partial^{\mu_l} \boldsymbol{\pi} + H.c.; \quad (7)$$

$$H(S\pi\pi) = \frac{1}{2} g_{S\pi\pi} S_{\mu_1 \dots \mu_J} (\boldsymbol{\pi} \cdot \partial^{\mu_1} \dots \partial^{\mu_J} \boldsymbol{\pi}) ; \quad (8)$$

$$\begin{aligned} H(SNN) = & \left[ g_{NNS}^{(1)} \overline{N} \partial_{\mu_1} \dots \partial_{\mu_J} N \right. \\ & \left. + ig_{NNS}^{(2)} J \partial_{\mu_1} \dots \partial_{\mu_{J-1}} \overline{N} \gamma_{\mu_J} N \right] S^{\mu_1 \dots \mu_J} \end{aligned} \quad (9)$$

$$H(V\pi\pi) = \frac{1}{2} g_{V\pi\pi} \mathbf{V}_{\mu_1 \dots \mu_J} (\boldsymbol{\pi} \times \partial^{\mu_1} \dots \partial^{\mu_J} \boldsymbol{\pi}) ; \quad (10)$$

$$\begin{aligned} H(VNN) = & \left[ ig_{NNV}^{(1)} \overline{N} \boldsymbol{\sigma} \partial_{\mu_1} \dots \partial_{\mu_J} N \right. \\ & \left. + g_{NNV}^{(2)} J \overline{N} \gamma_{\mu_J} \boldsymbol{\sigma} \partial_{\mu_1} \dots \partial_{\mu_{J-1}} N \right] \mathbf{V}^{\mu_1 \dots \mu_J} . \end{aligned} \quad (11)$$

In Eqs. (6, 7)  $P_{3/2}$  denotes the isospin-3/2 projecting operator:

$$\begin{aligned} P_{3/2} \equiv (P_{3/2})_{a\alpha b\beta} = & \frac{2}{3} \left\{ \delta_{\alpha\beta} \delta_{ab} - \frac{i}{2} \varepsilon_{abc} (\sigma_c)_{\alpha\beta} \right\}, \\ & (a, b = 1, 2, 3; \alpha, \beta = 1, 2). \end{aligned} \quad (12)$$

One can easily check that in momentum space these monomials provide the full set of 3-leg minimal vertices under the condition that the independent variables are chosen as  $p_n^2$  where  $p_n$  ( $n = 1, 2, 3$ ) stands for the 4-momentum of  $n$ th leg.



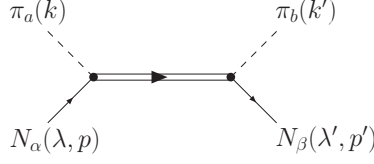


FIG. 2: Typical graph with a fermion resonance exchange. Here  $a, b, \alpha, \beta$  stand for isotopic indices and  $\lambda, \lambda'$  — for nucleon polarizations.

The 0th level coupling constants that appear in equations (4) – (11) are real. According to the results of [2] listed in Section II these couplings present the fundamental physical observables.

The general form of the minimal propagator of a particle with mass parameter  $M$  and spin number  $l$  (this corresponds to spin  $J = l$  for boson and  $J = l + 1/2$  for fermion) looks as follows:

$$P_{\nu_1 \dots \nu_l}^{\mu_1 \dots \mu_l}(q; l) = \frac{i}{(2\pi)^4} \frac{\Pi_{\nu_1 \dots \nu_l}^{\mu_1 \dots \mu_l}(q; l)}{q^2 - M^2 + i\epsilon} . \quad (13)$$

Here  $\Pi_{\nu_1 \dots \nu_l}^{\mu_1 \dots \mu_l}(q; l)$  is the relevant spin sum constructed from the Rarita-Schwinger wave functions  $\mathcal{E}^{\mu_1 \dots \mu_l}(i, p)$  and defined in (A1) for bosons and in (A6) for baryons. The eventual spinor indices and isotopic factors like  $\delta_{ab}$ ,  $\delta_{\alpha\beta}$  and  $P_{3/2}^{a\alpha b\beta}$  are omitted. The main properties of such spin sums are summarized in the Appendix A.

Now we have in hand all the ingredients needed to calculate those elements of tree level graphs which are used for constructing the Cauchy forms. In the next Section we explain certain specific details of the computational procedure.

#### IV. RESONANCE EXCHANGE GRAPH: EXAMPLE OF COMPUTATION

To construct the Cauchy forms for the scalar amplitudes  $A^\pm$  and  $B^\pm$  in (3), one needs to know the residues at the relevant resonance poles. Below we demonstrate how the contracted projector formalism (briefly reviewed in Appendix A) allows one to compute the contributions to these residues that follow from graphs with arbitrary spin resonance<sup>3</sup> exchanges.

As an example, consider the graph (Fig. 2) corresponding to the  $s$ -channel exchange by a resonance with spin  $J = l + 1/2$ , isospin  $I = 1/2$  and negative normality  $\mathcal{N} = -1$ .

---

<sup>3</sup> When speaking about internal lines we often use the term “resonance” for both stable and unstable particles.

The left and right resultant vertices are easily read from (5). They are, respectively,

$$-i g_{\hat{R}}^* (-i)^l k^{\nu_1} \dots k^{\nu_l} (\sigma_a)_{\gamma\alpha} \quad (14)$$

and

$$-i g_{\hat{R}} (i)^l k'_{\mu_1} \dots k'_{\mu_l} (\sigma_b)_{\beta\gamma} \quad (15)$$

( $\gamma = 1, 2$  is the isotopic index of the resonance). The corresponding minimal propagator is given by the expression (13) with  $l = J - 1/2$  ( $\rho, \tau$  stand for spinor indices and  $M$  – for the resonance mass parameter).

With the help of (13), (14), (15) and (A7) one can write down the contribution of the resultant graph shown on Fig. 2 to the amplitude of elastic pion-nucleon scattering as follows:

$$\begin{aligned} G_{b\beta a\alpha}(p, k, \lambda; p', k', \lambda') = \\ (\sigma_b \sigma_a)_{\beta\alpha} g_{\hat{R}}^* g_{\hat{R}} \bar{u}(p', \lambda') \mathcal{P}^{(l+\frac{1}{2})}(k', k, k+p) u(p, \lambda), \end{aligned} \quad (16)$$

where  $u(p, \lambda)$  and  $\bar{u}(p', \lambda')$  stand for the nucleon wave functions and  $\mathcal{P}^{(l+\frac{1}{2})}(k', k, k+p)$  — for contracted projector. Finally, using the explicit form (A8) of the contracted projector, one obtains the following expression for the contribution of the graph under consideration:

$$G_{b\beta a\alpha}(\dots) = -\frac{G(\pi N \hat{R})}{s - M_{\hat{R}}^2} (\sigma_b \sigma_a)_{\beta\alpha} \bar{u}(p', \lambda') \left[ F_A^l(M, t) + \frac{(\not{k} + \not{k}')}{2} F_B^l(M, t) \right] u(p, \lambda). \quad (17)$$

Here

$$G(\pi N \hat{R}) \equiv |g_{\hat{R}}|^2 \Phi^l \frac{l!}{(2l+1)!!}, \quad (18)$$

$$\begin{aligned} \Phi(M, m, \mu) \equiv \\ \frac{1}{4M^2} (M^4 + m^4 + \mu^4 - 2M^2 m^2 - 2M^2 \mu^2 - 2m^2 \mu^2), \end{aligned} \quad (19)$$

and  $m, \mu$  stand for the nucleon and pion mass, respectively. Two auxiliary functions  $F_A^l(M, t)$  and  $F_B^l(M, t)$  are defined as follows:

$$\begin{aligned} F_A^l(M, t) \equiv & (M + m) P'_{l+1} \left( 1 + \frac{t}{2\Phi} \right) \\ & + (M - m) \frac{(M + m)^2 - \mu^2}{(M - m)^2 - \mu^2} P'_l \left( 1 + \frac{t}{2\Phi} \right), \end{aligned} \quad (20)$$

$$F_B^l(M, t) \equiv P'_{l+1} \left( 1 + \frac{t}{2\Phi} \right) - \frac{(M+m)^2 - \mu^2}{(M-m)^2 - \mu^2} P'_l \left( 1 + \frac{t}{2\Phi} \right) . \quad (21)$$

Comparing now (17) with (2) and using the well known relation for Pauli matrices

$$(\sigma_b \sigma_a)_{\beta\alpha} = \delta_{ba} \delta_{\beta\alpha} + i \varepsilon_{bac} (\sigma_c)_{\beta\alpha} ,$$

we conclude that the graph on Fig. 2 gives the following contributions to the singular (or, the same, *principal*) parts of invariant amplitudes:

$$\begin{aligned} \text{to } A^+ : & \quad - \frac{G(\pi N \widehat{R})}{s - M_{\widehat{R}}^2} F_A^l(M, t) , \\ \text{to } A^- : & \quad - \frac{G(\pi N \widehat{R})}{s - M_{\widehat{R}}^2} F_A^l(M, t) , \\ \text{to } B^+ : & \quad - \frac{G(\pi N \widehat{R})}{s - M_{\widehat{R}}^2} F_B^l(M, t) , \\ \text{to } B^- : & \quad - \frac{G(\pi N \widehat{R})}{s - M_{\widehat{R}}^2} F_B^l(M, t) . \end{aligned}$$

In the same way, using the relations (A4) and (A8) one can derive expressions for all the other resultant graphs which correspond to a resonance exchange in one of the channels (see Fig. 1). The results are listed in Appendix B. This fixes the principal parts of tree level invariant amplitudes.

## V. CONSTRUCTING THE CAUCHY FORMS

In this Section we construct the Cauchy forms for tree level amplitudes  $A^\pm$  and  $B^\pm$  in three hyperlayers  $B_s$ ,  $B_t$  and  $B_u$  (their projections on the Mandelstam plane are shown on Fig. 3).

To construct the Cauchy form presenting a given tree level amplitude in a certain hyperlayer, one needs to know the degree of relevant bounding polynomial, the configuration of poles, and the explicit expressions for corresponding residues. The location of poles is fixed (or, better, parameterized) with the help of the mass parameters  $M_i$ . The corresponding residues are listed in the Appendix B.

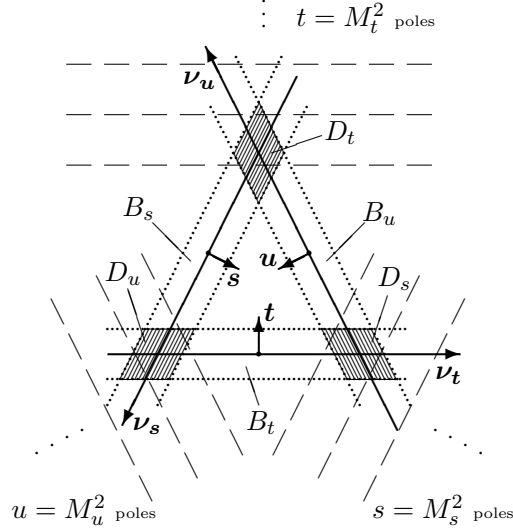


FIG. 3: Mandelstam plane: three different Cauchy series uniformly converge in three different hyperlayers  $B_s$ ,  $B_t$  and  $B_u$  (the projections are bounded by dotted lines). The intersection domains  $D_s$ ,  $D_t$ ,  $D_u$  are hatched. The dashed lines show the pole positions in the relevant channels.

The bounding polynomial degrees are chosen in accordance with known values of corresponding Regge intercepts (see Sec. II). In all the cases we have already examined ( $\pi\pi$ ,  $\pi K$ ,  $\pi N$ , and  $KN$  elastic scattering processes) it happens impossible to obtain reasonable (at least, roughly corresponding to known data) bootstrap conditions until this requirement is fulfilled. In the reaction under consideration the intercepts are (see e.g. [14]):

$$\alpha_0^M = 1; \quad \alpha_1^M \sim 0.5; \quad \alpha_{1/2}^B \sim 0; \quad \alpha_{3/2}^B < 0; \quad (22)$$

(here the upper indices M and B correspond to meson and baryon trajectory, respectively, while the lower ones refer to the isospin value). Using the numerical values (22) we conclude that:

- in  $B_s$ :

$$\begin{aligned} (A^+ + 2A^-) \Big|_{|\nu_s| \rightarrow \infty} &\sim O\left(\frac{1}{|\nu_s|}\right), \\ (B^+ + 2B^-) \Big|_{|\nu_s| \rightarrow \infty} &\sim O\left(\frac{1}{|\nu_s|}\right); \end{aligned} \quad (23)$$

$$\begin{aligned} (A^+ - A^-) \Big|_{|\nu_s| \rightarrow \infty} &\sim o\left(\frac{1}{|\nu_s|}\right), \\ (B^+ - B^-) \Big|_{|\nu_s| \rightarrow \infty} &\sim o\left(\frac{1}{|\nu_s|}\right); \end{aligned} \quad (24)$$

• in  $B_t$ :

$$\begin{aligned} (A^+) \Big|_{|\nu_t| \rightarrow \infty} &\sim o(|\nu_t|^2) , \\ (B^+) \Big|_{|\nu_s| \rightarrow \infty} &\sim O(1) ; \end{aligned} \tag{25}$$

$$\begin{aligned} (A^-) \Big|_{|\nu_t| \rightarrow \infty} &\sim o(|\nu_t|) , \\ (B^-) \Big|_{|\nu_s| \rightarrow \infty} &\sim o(1) ; \end{aligned} \tag{26}$$

• in  $B_u$ :

$$\begin{aligned} (A^+ - 2A^-) \Big|_{|\nu_s| \rightarrow \infty} &\sim o(1) , \\ (B^+ - 2B^-) \Big|_{|\nu_s| \rightarrow \infty} &\sim o(1) ; \end{aligned} \tag{27}$$

$$\begin{aligned} (A^+ - A^-) \Big|_{|\nu_s| \rightarrow \infty} &\sim o(1) , \\ (B^+ - B^-) \Big|_{|\nu_s| \rightarrow \infty} &\sim o(1) . \end{aligned} \tag{28}$$

Thus in  $B_s$  and  $B_u$  the invariant amplitudes  $A^\pm$  and  $B^\pm$  possess decreasing asymptotics. Therefore (see [2]) one does not need to take account of any correcting polynomials and subtraction terms in the Cauchy forms valid in these layers. The same is true with respect to  $B^-$  in  $B_t$ . Next, since  $A^-$  and  $B^+$  are odd functions of  $\nu_t$  (this is just a consequence of Bose symmetry), the zero degree is ruled out here and the correcting polynomials can also be dropped as well as the subtraction terms. At last, because  $A^+$  is even in  $B_t$ , the equation (25) tells us that the degree of corresponding bounding polynomial is zero.

We conclude that the only Cauchy form which requires taking account of (0th order in  $\nu_x$ ) correcting polynomials and the corresponding subtraction term is that representing the invariant amplitude  $A^+(t, \nu_t)$  in the hyperlayer  $B_t$ . In all other cases neither background terms nor correcting polynomials are needed; the corresponding Cauchy series are just the properly ordered sums of pole terms stemming from the relevant resultant graphs.

Now we can construct the Cauchy forms which provide the uniformly converging series for invariant amplitudes  $A^\pm$  and  $B^\pm$  in three hyperlayers  $B_s$ ,  $B_t$  and  $B_u$ . However, the explicit expressions are too bulky. To make them readable we need to introduce more compact notations.

Henceforth  $X^\pm$  stands for  $A^\pm$  or  $B^\pm$ ,  $M$  denotes the relevant resonance (baryon or meson) mass parameter and, as usual,  $m$  ( $\mu$ ) is the nucleon (pion) mass. Further, introducing the abbreviation

$$C_I^\pm : \{C_{1/2}^+ = 1; C_{1/2}^- = 1; C_{3/2}^+ = 2/3; C_{3/2}^- = -1/3\}, \quad (29)$$

we define for baryons

$$Y_X^\pm(M, \chi) \equiv \sum_{\substack{I=1/2, 3/2 \\ J=1/2, 3/2, \dots}} C_I^\pm G(\pi N \mathcal{R}) F_X^I(-\mathcal{N}M, \chi), \quad (30)$$

where  $\chi$  stands for arbitrary kinematical variable and  $\mathcal{N}$  – for normality, the summation being implied over all baryon resonances ( $\mathcal{R} = R, \widehat{R}, \Delta, \widehat{\Delta}$ ) with the same mass  $M$ . Similarly, for mesons:

$$W_X^\pm(M, \chi) \equiv \sum_{\substack{I=0,1 \\ J=0,1,\dots}} \frac{1}{2} [1 \pm (-1)^I] W_X(I, J, \chi), \quad (31)$$

where

$$\begin{aligned} W_A(I, J, \chi) \equiv & \frac{1}{2} [(-1)^I + (-1)^J] \\ & \times \left\{ G_1^I P_J(\chi) - \frac{4m}{4m^2 - M^2} G_2^I P'_{J-1}(\chi) \right\}, \end{aligned} \quad (32)$$

$$W_B(I, J, \chi) \equiv \frac{1}{2} [(-1)^I + (-1)^J] \frac{1}{F} G_2^I P'_J(\chi). \quad (33)$$

In the Eq. (31) the summation<sup>4</sup> is implied over all non-strange meson resonances with the same mass  $M$  and natural parity  $P = (-1)^J$ . Finally, introducing the sign regulator

$$\eta_X = \begin{cases} +1, & X = A \\ -1, & X = B \end{cases} \quad (34)$$

and abbreviations

$$\Sigma \equiv [M^2 - 2(m^2 + \mu^2)], \quad \theta \equiv (M^2 - m^2 - \mu^2), \quad (35)$$

we can write down the compact expressions for desired Cauchy forms.

---

<sup>4</sup> Both sums in (30) and (31) are *finite* because, as mentioned in Sec. III, we imply that the number of resonances with the same value of mass parameter is finite. To put it another way, we imply existence of the leading Regge trajectory (in the plane  $(J, M)$ ) which, however, is not necessarily linear.

- $B_s\{\nu_s \in \mathbb{C}; s \in \mathbb{R}, s \sim 0\}$ .

Here the relevant poles are those in  $t$  and  $u$ . The asymptotic behavior of every invariant amplitude  $A^\pm(s, \nu_s)$  and  $B^\pm(s, \nu_s)$  in  $\nu_s$  corresponds to the negative degree of bounding polynomial. Thus we see that each one of these amplitudes can be presented as follows ( $X = A, B$ ):

$$\begin{aligned} X^\pm \Big|_{B_s} &= (\pm \eta_X) \sum_{\text{baryons}} Y_X^\pm \left( M, -(\Sigma + s) \right) \frac{-2}{\nu_s - (s + 2\theta)} \\ &\quad + \sum_{\text{mesons}} W_X^\pm \left( M, \frac{\Sigma + 2s}{4F} \right) \frac{2}{\nu_s + (s + 2\theta)} . \end{aligned} \quad (36)$$

- $B_t\{\nu_t \in \mathbb{C}; t \in \mathbb{R}, t \sim 0\}$ .

As mentioned above, in this hyperlayer the amplitude  $A^+$  requires accounting for the 0th degree correcting polynomials and subtraction term. With the latter term denoted as  $\alpha(t)$  the correct Cauchy form reads:

$$\begin{aligned} A^+ \Big|_{B_t} &= \alpha(t) - \sum_{\text{baryons}} Y_A^+(M, t) \left[ \frac{2}{\nu_t - (t + 2\theta)} \right. \\ &\quad \left. - \frac{2}{\nu_t + (t + 2\theta)} + \frac{4}{t + 2\theta} \right] . \end{aligned} \quad (37)$$

At the same time, the amplitudes  $A^-$  and  $B^\pm$  do not require accounting for correcting polynomials. Hence the relevant Cauchy forms read:

$$\begin{aligned} A^- \Big|_{B_t} &= - \sum_{\text{baryons}} Y_A^-(M, t) \left[ \frac{2}{\nu_t - (t + 2\theta)} - \frac{-2}{\nu_t + (t + 2\theta)} \right] , \\ B^\pm \Big|_{B_t} &= - \sum_{\text{baryons}} Y_B^\pm(M, t) \left[ \frac{2}{\nu_t - (t + 2\theta)} \mp \frac{-2}{\nu_t + (t + 2\theta)} \right] . \end{aligned} \quad (38)$$

- $B_u\{\nu_u \in \mathbb{C}; u \in \mathbb{R}, u \sim 0\}$ .

In this hyperlayer the situation is analogous to that in  $B_s$ . Thus we have ( $X = A, B$ ):

$$\begin{aligned} X^\pm \Big|_{B_u} &= - \sum_{\text{baryons}} Y_X^\pm \left( M, -(\Sigma + u) \right) \frac{-2}{\nu_u + (u + 2\theta)} \\ &\quad - \sum_{\text{mesons}} W_X^\pm \left( M, -\frac{\Sigma + 2u}{4F} \right) \frac{2}{\nu_u - (u + 2\theta)} . \end{aligned} \quad (39)$$

We would like to stress that all the sums over resonance contributions should be taken in order of increasing mass — otherwise the convergence of the Cauchy series cannot be guaranteed (see, e.g., [2]). The formal separation of these sums into meson and baryon parts is done just to show the explicit form of both kinds of contributions.

Before proceeding further it is useful to summarize briefly what has been done up to this moment.

First, we performed the classification of all the minimal triple vertices that describe the interaction of pions and nucleons with meson and baryon resonances of arbitrary high spin  $J$  and isospin  $I \leq 3/2$ .

Second, we have calculated the explicit form of the residues at poles stemming from graphs that correspond to resonance exchanges in one of three channels of the considered process. This allowed us to separate the full collection of contributions from the tree level graphs (Fig. 1) into two *formal* infinite sums, the first one being solely constructed from the pole terms while the second is a (formal) power series in arbitrary pair of independent kinematical variables  $(x, \nu_x)$ .

Third, following the procedure proposed in [1, 2] (and suggestions listed in Sec. II), we constructed the uniformly converging Cauchy series (36) – (39) which provide the correct forms of invariant amplitudes in three hyperlayers  $B_x$ . Let us stress that these series are constructed from the well-defined expressions, the only item still unspecified being the subtraction term  $\alpha(t)$  that appears in (37).

The important feature of the Cauchy forms (36) – (39) is that, as a rule, neither poles in  $x$  nor smooth (‘background’) terms depending on both variables  $(x, \nu_x)$  appear explicitly in a form valid in  $B_x$ . The only exception is the Cauchy form (37) for  $A^+$  in  $B_t$ . It contains the background term  $\alpha(t)$  depending on  $t$ . This means that there must exist a mutual cancellation between the direct channel background terms and the cross channel poles, this cancellation being complete in all the hyperlayers except  $B_t$ . In this latter case the remnant of cross channel poles and background contributions survives in the amplitude  $A^+(t, \nu_t)$ . It manifests itself in a form of (still unspecified) subtraction term  $\alpha(t)$  and an infinite number of well-defined smooth terms (the correcting polynomials) that appear in each item of the sum over pole contributions.

Such a cancellation might seem a miracle if ever possible since it requires extremely fine tuning of the structure of a set of resultant parameters. Fortunately, there exists an example



which allows one to trace the mechanism of this phenomenon — the famous string amplitude based on Euler’s B-function. This example has been analyzed in [3, 5]. It was shown that the corresponding bootstrap conditions present nothing but an infinite set of identities for Pochhammer symbols which easily undergo numerical verification.

For this reason it is interesting to construct the explicit form of bootstrap conditions for  $\pi N$  scattering amplitude and compare them with known data. As mentioned above, this may provide a test of consistency of the set of requirements listed in Sec. II.

## VI. BOOTSTRAP CONDITIONS

According to the analysis presented in [1]-[3], the full system of bootstrap restrictions is a system of necessary conditions limiting the values of resultant parameters of various levels. This system ensures self-consistency of the effective theory in  $S$ -matrix sector. It arises as a direct consequence of the summability principle.

Below we consider only a small (though infinite!) part of this system. Namely, we derive the *tree level bootstrap restrictions* for the resultant parameters of  $\pi N$  scattering (masses and triple coupling constants that appear in (4) – (11)). As argued in [2], the bootstrap conditions possess the property of renormalization invariance: irrelatively to their loop level, they restrict the possible values of physical observables in a given effective theory. It is for this reason that already the tree-level bootstrap conditions can be verified by the direct comparison with experimental data.

First of all let us derive the bootstrap condition which allows one to express the unknown function  $\alpha(t)$  (see Eq. (37)) in terms of triple couplings and masses. It follows from the existence of *two* Cauchy forms (namely, (37) and (39)) which present the same function  $A^+$ , both forms being valid in the domain  $D_s = B_u \cap B_t$ . Hence in this domain they must coincide identically. This gives:

$$\begin{aligned} \alpha(t) = & \sum_{\text{baryons}} \left\{ \frac{Y_A^+(M, -(u + \Sigma)) - Y_A^+(M, t)}{\Sigma + t + u} + Y_A^+(M, t) \left[ \frac{1}{u - M^2} + \frac{4}{t + 2\theta} \right] \right\} \\ & - \sum_{\text{mesons}} W_A^+ \left( M, -\frac{(2u + \Sigma)}{4F} \right) \frac{1}{t - M^2} \equiv \Psi_s(A^+); \quad (t, u) \in D_s. \end{aligned} \quad (40)$$

Here we have used (1) to express  $\nu_t$  and  $\nu_u$  in terms of  $(t, u)$ . In [2] the relations of the type

(40) have been called as the bootstrap conditions of the first kind.

As we have already mentioned in Sec. V,  $\alpha(t)$  (as well as the correcting polynomials) results from the contributions of contact (pointlike) graphs and from the graphs with  $t$ -channel resonance exchanges. Nevertheless, the right side of (40) only depends on the tree level resultant coupling constants at triple vertices. Thus the relation (40) gives an illustration to the general statement made in [2]: there is no need to formulate the independent renormalization prescriptions for 4-leg amplitudes as long as the true (experimental) asymptotic behavior is taken into account in our scheme.

The formula (40) is only valid in  $D_s$ ; outside this domain it is meaningless because at least one of two series (37), (39) may diverge. For this reason the pole terms which appear in the right side, in fact, do not correspond to singularities — the function  $\alpha(t)$  is smooth in  $D_s$ . Moreover, since it only may depend on  $t$ , the expression (40) defines this function everywhere in the hyperlayer  $B_t$  *under the condition that the parameters fulfil certain self-consistency restrictions which provide a guarantee of independence of the right side on the variable  $u$* . In the case under consideration these restrictions may be written as follows<sup>5</sup>:

$$\partial_u^{m+1} \partial_t^n \Psi_s(A^+) \Big|_{t,u=0} = 0, \quad (m, n = 0, 1, \dots). \quad (41)$$

The infinite system of equations (41) only contains the numerical parameters<sup>6</sup> — the resultant triple coupling constants and masses. It provides an example of sum rules that connect among themselves the parameters of fermion and boson spectra.

Clearly, the system (41) presents only one of necessary self-consistency conditions. Indeed, there are three domains where two of three hyperlayers ( $B_s$ ,  $B_t$  and  $B_u$ ) intersect:

$$D_s = B_t \cap B_u; \quad D_t = B_u \cap B_s; \quad D_u = B_s \cap B_t.$$

Therefore, we have three systems of such functional self-consistency conditions, namely:

$$A^\pm \Big|_{B_t} = A^\pm \Big|_{B_u}, \quad B^\pm \Big|_{B_t} = B^\pm \Big|_{B_u}, \quad (t, u) \in D_s; \quad (42)$$

$$A^\pm \Big|_{B_u} = A^\pm \Big|_{B_s}, \quad B^\pm \Big|_{B_u} = B^\pm \Big|_{B_s}, \quad (u, s) \in D_t; \quad (43)$$

---

<sup>5</sup> Here the reference point  $(t, u) = (0, 0)$  is chosen just for convenience; in principle, every point  $(t, u) \in D_s$  would be equally acceptable.

<sup>6</sup> In [2] the systems of this type are called as the second kind bootstrap conditions.

$$A^\pm \Big|_{Bs} = A^\pm \Big|_{Bt}, \quad B^\pm \Big|_{Bs} = B^\pm \Big|_{Bt}, \quad (s, t) \in D_u. \quad (44)$$

Obviously in the case of  $\pi N$  elastic scattering the systems (44) and (42) are completely equivalent. For this reason it is quite sufficient to consider only two systems: (42) and (43). It is convenient to present them in terms of two groups of generating functions.

The functions from the first group generate the self-consistency (bootstrap) conditions (42). We define them as follows<sup>7</sup>:

$$\begin{aligned} \Psi_s(A^+) \equiv & \sum_{\text{baryons}} \left\{ \frac{Y_A^+(M, -(u + \Sigma)) - Y_A^+(M, t)}{\Sigma + t + u} + Y_A^+(M, t) \left[ \frac{1}{u - M^2} + \frac{4}{t + 2\theta} \right] \right\} \\ & - \sum_{\text{mesons}} \frac{W_A^+(M, -(2u + \Sigma)/4F)}{t - M^2}; \end{aligned} \quad (45)$$

$$\begin{aligned} \Psi_s(A^-) \equiv & \sum_{\text{baryons}} \left\{ \frac{Y_A^-(M, -(u + \Sigma)) - Y_A^-(M, t)}{\Sigma + t + u} - \frac{Y_A^-(M, t)}{u - M^2} \right\} \\ & - \sum_{\text{mesons}} \frac{W_A^-(M, -(2u + \Sigma)/4F)}{t - M^2}; \end{aligned} \quad (46)$$

$$\begin{aligned} \Psi_s(B^+) \equiv & \sum_{\text{baryons}} \left\{ \frac{Y_B^+(M, -(u + \Sigma)) - Y_B^+(M, t)}{\Sigma + t + u} - \frac{Y_B^+(M, t)}{u - M^2} \right\} \\ & - \sum_{\text{mesons}} \frac{W_B^+(M, -(2u + \Sigma)/4F)}{t - M^2}; \end{aligned} \quad (47)$$

$$\begin{aligned} \Psi_s(B^-) \equiv & \sum_{\text{baryons}} \left\{ \frac{Y_B^-(M, -(u + \Sigma)) - Y_B^-(M, t)}{\Sigma + t + u} + \frac{Y_B^-(M, t)}{u - M^2} \right\} \\ & - \sum_{\text{mesons}} \frac{W_B^-(M, -(2u + \Sigma)/4F)}{t - M^2}. \end{aligned} \quad (48)$$

The corresponding bootstrap conditions read:

$$\partial_t^m \partial_u^{n+1} \Psi_s(A^+) \Big|_{t,u=0} = 0, \quad (m, n = 0, 1, \dots); \quad (49)$$

$$\begin{aligned} \partial_t^m \partial_u^n \Psi_s(X_s) \Big|_{t=u=0} &= 0, \\ (m, n = 0, 1, \dots). \quad (X = A^-, B^+, B^-). \end{aligned} \quad (50)$$

Similarly, the second group of generating functions is defined as:

---

<sup>7</sup> Except  $\Psi_s(A^+)$ , all these functions are just the differences of two relevant Cauchy forms.

$$\begin{aligned}\Psi_t(A^+) \equiv & \sum_{\text{baryons}} \left[ \frac{Y_A^+(M, -(u + \Sigma))}{s - M^2} - \frac{Y_A^+(M, -(s + \Sigma))}{u - M^2} \right] \\ & - \sum_{\text{mesons}} \frac{W_A^+(M, -(2u + \Sigma)/4F) - W_A^+(M, (2s + \Sigma)/4F)}{\Sigma + s + u};\end{aligned}\quad (51)$$

$$\begin{aligned}\Psi_t(A^-) \equiv & \sum_{\text{baryons}} \left[ \frac{Y_A^-(M, -(u + \Sigma))}{s - M^2} + \frac{Y_A^-(M, -(s + \Sigma))}{u - M^2} \right] \\ & - \sum_{\text{mesons}} \frac{W_A^-(M, -(2u + \Sigma)/4F) - W_A^-(M, (2s + \Sigma)/4F)}{\Sigma + s + u};\end{aligned}\quad (52)$$

$$\begin{aligned}\Psi_t(B^+) \equiv & \sum_{\text{baryons}} \left[ \frac{Y_B^+(M, -(u + \Sigma))}{s - M^2} + \frac{Y_B^+(M, -(s + \Sigma))}{u - M^2} \right] \\ & - \sum_{\text{mesons}} \frac{W_B^+(M, -(2u + \Sigma)/4F) - W_B^+(M, (2s + \Sigma)/4F)}{\Sigma + s + u};\end{aligned}\quad (53)$$

$$\begin{aligned}\Psi_t(B^-) \equiv & \sum_{\text{baryons}} \left[ \frac{Y_B^-(M, -(u + \Sigma))}{s - M^2} - \frac{Y_B^-(M, -(s + \Sigma))}{u - M^2} \right] \\ & - \sum_{\text{mesons}} \frac{W_B^-(M, -(2u + \Sigma)/4F) - W_B^-(M, (2s + \Sigma)/4F)}{\Sigma + s + u}.\end{aligned}\quad (54)$$

These functions generate the bootstrap conditions (43):

$$\begin{aligned}\partial_u^m \partial_s^n \Psi_t(X_t) \Big|_{u=s=0} &= 0, \\ (m, n = 0, 1, \dots), \quad (X = A^\pm, B^\pm).\end{aligned}\quad (55)$$

It should be stressed once more that the expansion points  $(t, u) = (0, 0)$  and  $(s, u) = (0, 0)$  in Eqs. (49), (50) and (55) are chosen just for convenience. Any other point from the corresponding domains would be equally acceptable.

As it was already emphasized, the bootstrap constraints restrict the allowed values of the physical (experimentally observable) parameters. This is true with respect to the constraints of arbitrary level, and in particular, with respect to tree level ones. Therefore, the direct comparison of the constraints (49), (50), (55) with known data is quite allowable. Unfortunately, the modern data on the resonance spectrum are far from being complete. Nevertheless, in two subsequent Sections we will show that it is possible to choose certain subsystem of constraints under consideration such that the total contribution from heavy resonances turns out small due to rapid convergence of the relevant series.

## VII. SUM RULES FOR $\rho$ -MESON COUPLING CONSTANTS

In this Section we perform the detailed numerical analysis of two particular bootstrap constraints (sum rules) that connect among themselves the parameters of baryon and meson spectra. This allows us to demonstrate an astonishing balance between the numerical values of two  $\rho NN$  physical coupling constants  $G_{NN\rho}^T$  and  $G_{NN\rho}^V$  and (also physical) parameters of the baryon spectrum.

The quantities  $G_{NN\rho}^T$  and  $G_{NN\rho}^V$  are defined (see [8]) as coupling constants in the effective Hamiltonian (below  $\sigma_{\mu\nu} \equiv -\frac{i}{4}[\gamma_\mu, \gamma_\nu]$ )

$$H_{\text{eff}}^{NN\rho} = -\overline{N} \left[ G_{NN\rho}^V \gamma_\mu \boldsymbol{\rho}^\mu - G_{NN\rho}^T \frac{\sigma_{\mu\nu}}{4m} (\partial^\mu \boldsymbol{\rho}^\nu - \partial^\nu \boldsymbol{\rho}^\mu) \right] \frac{1}{2} \boldsymbol{\sigma} \cdot \mathbf{N} . \quad (56)$$

Our constants  $g_{NN\rho}^{(1)}$  and  $g_{NN\rho}^{(2)}$  introduced in (11) are related to  $G_{NN\rho}^V$  and  $G_{NN\rho}^T$  as follows:

$$g_{NN\rho}^{(1)} \equiv \frac{1}{2m} G_{NN\rho}^T ,$$

$$g_{NN\rho}^{(2)} \equiv \frac{G_{NN\rho}^V - G_{NN\rho}^T}{2} ,$$

and  $G_{\pi\pi\rho}$  defined in [8] differs from our one by the factor of 2:

$$g_{\rho\pi\pi} \equiv 2G_{\pi\pi\rho} .$$

The existing experimental data (see [8]) give:

$$\frac{G_{NN\rho}^T}{G_{NN\rho}^V} \approx 6.1 \pm 0.6 , \quad \frac{G_{\pi\pi\rho} G_{NN\rho}^V}{4\pi} \approx 2.4 \pm 0.4 ,$$

$$G_{\pi\pi\rho} \approx 6.0 . \quad (57)$$

Let us now take  $\Psi_s(B^-)$  from (48),  $\Psi_t(A^-)$  from (52), and consider the forms (50), (55) at  $m, n = 0$  (i.e. without derivatives). This yields two numerical relations:

$$\sum_{\text{baryons}} \left\{ \frac{Y_B^-(M, -\Sigma) - Y_B^-(M, 0)}{\Sigma} - \frac{Y_B^-(M, 0)}{M^2} \right\} =$$

$$- \sum_{\substack{\text{mesons} \\ \text{with } I=1}} \frac{W_B^-(M, \Sigma/4F)}{M^2} ; \quad (58)$$

$$\sum_{\text{baryons}} \frac{Y_A^-(M, -\Sigma)}{M^2} = \sum_{\substack{\text{mesons} \\ \text{with } I=1}} \frac{W_A^-(M, \Sigma/4F)}{\Sigma} , \quad (59)$$

which can be compared with known data on resonance parameters. The  $\pi N$ -resonances with spin  $J = l + 1/2$ , ( $l = 0, 1, 2, \dots$ ) and isospin  $I = 1/2, 3/2$ , as well as the isovector  $\pi\pi$ -resonances with spin  $J = 1, 3, \dots$  contribute to these equations. It should be probably stressed again that the summation is performed in order of increasing mass regardless of the other quantum numbers of contributing resonances. As long as we can rely on existing experimental values of contributing parameters, both series above converge very fast. Actually, only four baryons ( $N(940)$ ,  $N(1440)$ ,  $N(1520)$  and  $\Delta(1232)$ ) and one meson ( $\rho(770)$ ) provide significant contributions. This allows one to neglect the heavier resonances when performing the numerical verification of sum rules under consideration.

Using the relations of Sec. V and the values (57) of three  $\rho$ -meson coupling constants  $G_{\pi\pi\rho}$ ,  $G_{NN\rho}^V$  and  $G_{NN\rho}^T$ , one can easily estimate the  $\rho$ -meson contributions to the right sides of (58) and (59). The values of baryon resonance parameters given in Appendix C allow one to do the same with respect to the left sides. In the case when we take account of all resonances with  $M_R \leq 1.52$  GeV in the baryon sector this results in the following numerical relations:

$$\text{Eq. (58) : } \quad 324.7 \pm 24 \approx 254 \pm 85;$$

$$\text{Eq. (59) : } \quad 42 \pm 6 \approx 50 \pm 12.5.$$

The uncertainties of right sides should not be taken too seriously — these numbers are just indicative (see [8] and references therein). In contrast, the left sides are estimated in accordance with the numbers given in Appendix C. As we just mentioned, the contributions from heavier baryon resonances turn out to be small, which gives a hope that the above series converges rapidly enough and eventual (yet unknown) heavy resonances will not change the sum considerably. This point is graphically illustrated in the next Section. One may see that both sum rules (58) and (59) are quite consistent with known data on the resonance spectrum, as long as the only resonances taken into account are baryons with masses  $M \leq 1.52$  GeV and the meson  $\rho(770)$ . This coincides well with the so-called *local cancellation hypothesis* (see the series of papers [16]).

What happens when the contributions from heavier resonances are included? In fact, the left side of sum rule (59) remains almost unchanged until the baryon resonance  $\Delta(1950)$  ( $J = 7/2$ ;  $\mathcal{N} = -1$ ) is taken into account. Its contribution slightly destroys the balance. As to the sum rule (58), the same phenomenon exhibits itself even earlier: already the

contribution from  $N(1680)$  ( $J = 5/2$ ;  $\mathcal{N} = +1$ ) results in small imbalance. In both cases the explanation is quite obvious: to treat the series correctly (in order of increasing mass) one needs to take account of the contributions from heavier meson resonances (in particular, from  $\rho(1450)$ ) in the right sides. Unfortunately, the modern experimental data on the relevant parameters of those resonances are insufficiently complete to make this possible.

We shall conclude that both bootstrap constraints (sum rules) (58) and (59) look quite reasonable from the modern experimental viewpoint. In particular, one can consider  $G_{NN\rho}^V$  and  $G_{NN\rho}^T$  as unknown parameters and get estimates for them from Eqs. (58), (59) (see, e.g., [6]). What is interesting to note, is that these constraints possess a supersymmetric feature — they connect among themselves the properties of meson and baryon spectra.

## VIII. NUMERICAL TESTING OF SUM RULES FOR $\pi N$ SPECTRUM PARAMETERS

In this Section we perform a more detailed numerical testing of the second kind bootstrap conditions (sum rules) (49), (50) and (55) for the parameters of pion-nucleon resonance spectrum.

We stress once more that in our effective scattering theory approach the system of bootstrap conditions (irrelevantly to their level) gives a set of constraints for the *physical values* of spectrum parameters. That is why the numerical testing of the tree level constraints is highly demanding: it allows one to check whether our scheme is applicable for realistic scattering processes.

The numerical testing of constraints in the toy bootstrap model (Lovelace string-like amplitude) was successfully carried out in [3]. In the case of pion-nucleon scattering the situation is a bit more complicated, since experimental information on resonances is incomplete — only the initial part of spectrum is relatively well established. This may cause certain problems because it is not known in advance whether a given sum rule converges sufficiently rapidly. Besides, the physical spectrum, as a rule, contains some poorly established resonances. The corresponding contributions to sum rules cannot be estimated with sufficient accuracy.

Nevertheless, as shown below, many of bootstrap constraints for the parameters of  $\pi N$  spectrum seem to converge sufficiently rapidly. In practice they are saturated by several

lightest well established resonances; the heavier ones just add small corrections.

To demonstrate the saturation we consider the balance of a given sum rule as a function of the heaviest resonance mass taken into account. For this we introduce partial sums of positive and negative contributions:  $S^+(M_R)$  and  $S^-(M_R)$ , respectively. For example, consider the sum rules which follow from the constraints (50) for the invariant amplitude  $A^-$  in  $D_s$  (the relevant generating function  $\Psi_s(A^-)$  is given in (46)). For particular  $m$  and  $n$  we define:

$$S^+(M) = \sum_{\substack{R_s R_t R_u, \\ M_R \leq M}} \frac{\partial^{m+n} \psi_s(A^-)}{\partial t^m \partial u^n} \bigg|_{\substack{t=0 \\ u=0}},$$

where every term  $\frac{\partial^{m+n} \psi_s(A^-)}{\partial t^m \partial u^n} \bigg|_{\substack{t=0 \\ u=0}} \geq 0;$

$$S^-(M) = \sum_{\substack{R_s R_t R_u, \\ M_R \leq M}} \left| \frac{\partial^{m+n} \psi_s(A^-)}{\partial t^m \partial u^n} \bigg|_{\substack{t=0 \\ u=0}} \right|,$$

where every term  $\frac{\partial^{m+n} \psi_s(A^-)}{\partial t^m \partial u^n} \bigg|_{\substack{t=0 \\ u=0}} < 0.$

Here  $\psi_s(A^-)$  is an individual resonance contribution to the generating function  $\Psi_s(A^-)$ . These notations allow one to present the sum rule under consideration as follows:

$$S^+(M) + \dots = S^-(M) + \dots,$$

where ellipses stand for the relevant contributions of resonances with  $M_R > M$ . Obviously, when  $S^+ \approx S^-$  the sum rule can be considered as a well saturated one. On Figures 4, 5, 6 we present several examples of the dependence of  $S^+$  and  $S^-$  on the mass of heaviest baryon resonance taken into account. The error bars for  $S^+$  and  $S^-$  originate mainly from the uncertainties of decay widths (or, the same, from those of triple  $\pi NR$  couplings). To make the domains of intersection of error bars better visible on our Figures 4 – 6 the error bars corresponding to  $S^-$  are shifted by 5 MeV to the right from the resonance position.

Some difficulties may arise if a sum rule gets significant contribution from the meson sector, because the spectrum of heavy non-strange mesons is known with much less precision than that of baryon resonances. In this case it makes sense to choose for numerical testing those sum rules which may only acquire contributions from meson resonances with  $I = 1$ . In many cases the contribution of well established  $\rho(770)$  meson turns out to be the dominant



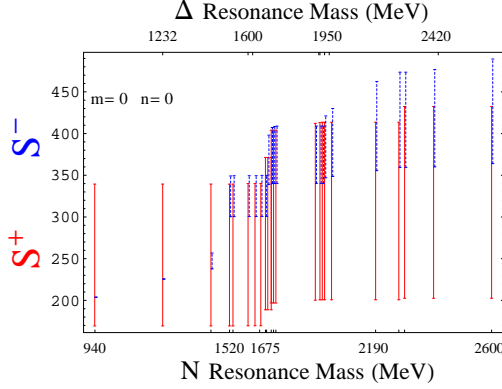


FIG. 4: Numerical testing of sum rule following from the bootstrap condition (50) for  $B^-$  in  $D_s$  at  $m = n = 0$ .

one. Two sum rules of this kind have been discussed in the previous Section. On the Figure 4 it is graphically shown the process of saturation of the bootstrap condition (50) at  $m = n = 0$ .

In this case the positive contribution of  $\rho(770)$  meson is compensated by the contributions from nucleon,  $\Delta(1232)$  and  $N(1440)$ . The contributions due to heavier baryon resonances seem to slightly disturb the balance. As noted above, this can be explained as a result of our poor knowledge of the contributions from baryons with  $M > 2$  GeV and from heavier mesons (say,  $\rho(1450)$ ).

Now let us consider the sum rules that follow from the bootstrap constraints (49), (50), (55) with derivatives (i.e.  $m, n \neq 0$ ). It is necessary to stress that the saturation of such sum rules requires attracting the more detailed information on spectrum because of the following reasons:

- The influence of heavy resonances with high spin becomes relatively more important. This is just because the differentiation kills the contributions of well established low spin resonances.
- The sum rules that arise from bootstrap conditions with derivatives in some cases converge slowly. This is explained by the fact that the resonances closest to the domain  $D_x$  under consideration may give significant contribution due to the presence of small parameter in the denominator. To compensate gradually their contributions one needs to take account of a large number of cross channel resonances. Such a situation was encountered during the numerical testing of sum rules in the toy bootstrap model for

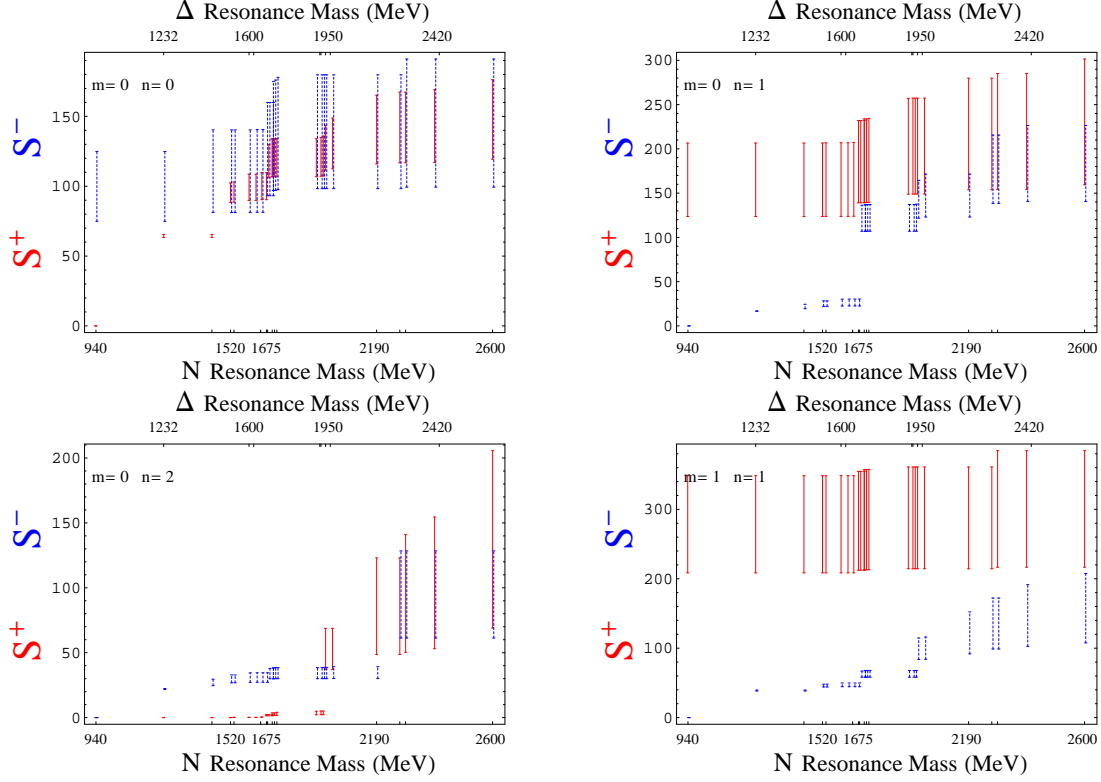


FIG. 5: Numerical testing of sum rules following from the bootstrap condition (50) for  $A^-$  in  $D_s$  for different values of  $m$  and  $n$ .

the Lovelace amplitude (see [3]).

However, it turns out possible to point out a series of the bootstrap constrains with derivatives that are reasonably well saturated with known experimental data. As an example of such sum rules let us consider several bootstrap conditions (50) for the invariant amplitude  $A^-$  at the domain  $D_s$ . The result of saturation of these sum rules for different values of  $m$  and  $n$  is presented on Figure 5. Note that these sum rules acquire contributions from  $I = 1$ ;  $J^P = 1^-, 3^-, \dots$  meson resonances while we only take into account that of  $\rho(770)$ .

As a second example we have chosen a series of purely baryon sum rules that follow from bootstrap constrains for the same invariant amplitude  $A^-$  in another intersection domain, namely, in  $D_t$ . The results are presented on Fig. 6. These sum rules (except that corresponding to  $m = n = 1$ ) can be considered as reasonably well saturated with known experimental data. It is interesting to notice that the similar situation was also encountered in the “toy bootstrap model” for Veneziano string amplitude [3]. In certain sum rules for resonance parameters of the string amplitude it was sufficient to take into account the contribution of a relatively small number of first poles to saturate it with high precision. At the

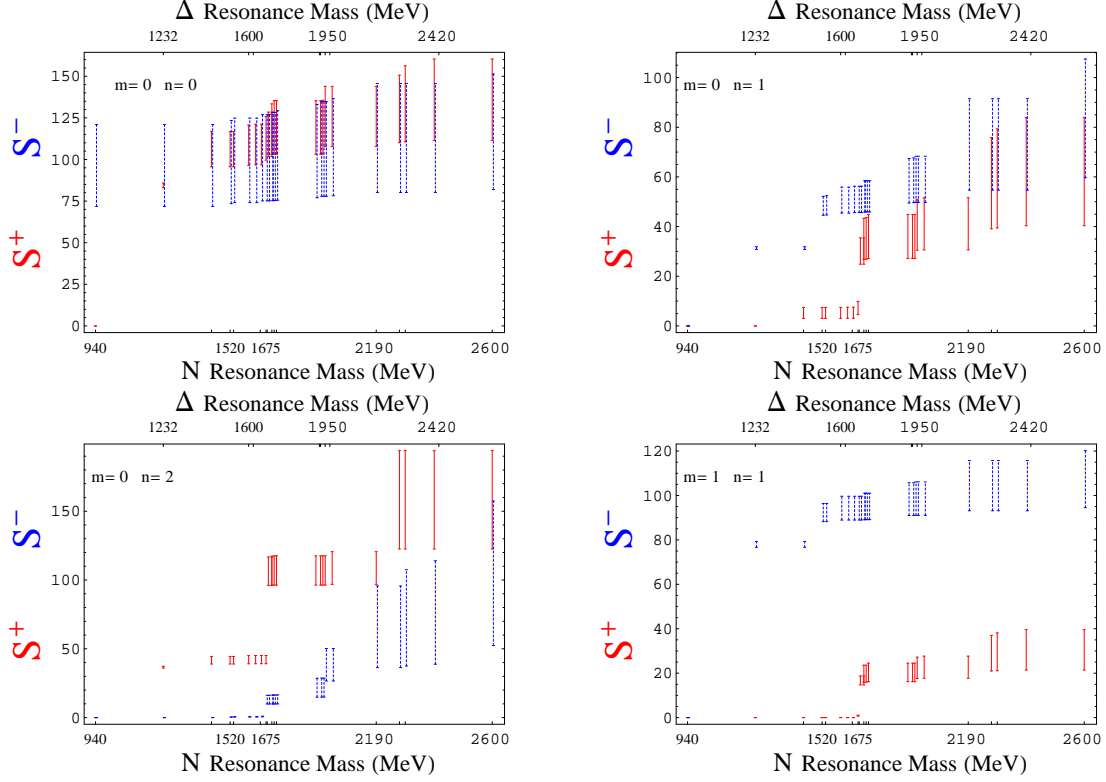


FIG. 6: Numerical tests of sum rules following from bootstrap condition (55) for the amplitude  $A^-$  in  $D_t$  at different values of  $m$  and  $n$ .

same time, in some other sum rules it was necessary to take into account the contribution of considerable number of poles to compensate the ‘accidentally large’ contribution coming from several first poles. A more detailed information on resonance spectrum is required to saturate slowly converging sum rules like (50) with  $m = n = 1$ .

Similar series of well saturating sum rules can also be derived from the bootstrap conditions for other invariant amplitudes ( $A^+$ ,  $B^\pm$ ) in the domains  $D_s$  and  $D_t$ . This is unlikely to be just an accidental luck. Instead, it gives serious arguments that the bootstrap constraints for pion-nucleon spectrum are supported by modern data. Since these constraints appear as the necessary consistency conditions in the extended perturbation scheme, this fact can be regarded as a strong evidence in favor of the latter one.

It is essential that the sum rules of this kind can be used as a powerful tool in studying the hadron resonance spectrum. This aspect will be discussed in more detail in the next paper devoted to the analysis of bootstrap constraints for the elastic kaon-nucleon scattering amplitude.

## IX. LOW-ENERGY COEFFICIENTS

In this Section we present our estimates for the expansion coefficients of tree level amplitudes around the cross-symmetric point ( $t = 0, \nu_t = 0$ ) in  $B_t$ . These results present certain interest because those coefficients undoubtedly do acquire contributions from the loop graphs. Nevertheless, as shown below, our estimates based on the tree level approximation of extended perturbation scheme turn out to be in nice agreement with the known data. This fact demonstrates that the latter scheme provides quite reasonable numbers already at tree level and, hence, may be of interest from the computational point of view.

Introducing the new quantity

$$C^\pm = A^\pm + \frac{m\nu_t}{4m^2 - t} \tilde{B}^\pm ,$$

(here  $\tilde{B}^\pm$  is just  $B^\pm$  with the nucleon pole subtracted<sup>8</sup>) we define the low-energy coefficients (LEC's)  $a_{mn}^\pm$ ,  $b_{mn}^\pm$ , and  $c_{mn}^\pm$  as those in double Taylor series expansions around the cross-symmetric point ( $t = 0, \nu_t = 0$ ):

$$\begin{aligned} \tilde{B}^+(t, \nu_t) &= \nu_t \sum_{m,n} b_{mn}^+ (\nu_t^2)^m t^n ; \\ \tilde{B}^-(t, \nu_t) &= \sum_{m,n} b_{mn}^- (\nu_t^2)^m t^n ; \\ A^+(t, \nu_t) &= \sum_{m,n} a_{mn}^+ (\nu_t^2)^m t^n ; \\ A^-(t, \nu_t) &= \nu_t \sum_{m,n} a_{mn}^- (\nu_t^2)^m t^n ; \\ C^+(t, \nu_t) &= \sum_{m,n} c_{mn}^+ (\nu_t^2)^m t^n ; \\ C^-(t, \nu_t) &= \nu_t \sum_{m,n} c_{mn}^- (\nu_t^2)^m t^n . \end{aligned}$$

To get numerical values for these coefficients, we need to re-expand the Cauchy forms (37), (38) and (40) in double power series in  $(t, \nu_t)$ . This is quite admissible because these forms converge uniformly in whole  $B_t$  and, therefore, near the cross-symmetric point.

Now, using the data [8], [15] (see also the Table in Appendix C) on coupling constants and masses and neglecting the contributions of resonances with  $M \geq 1.95$  GeV, one can get

---

<sup>8</sup> At this point we follow the definitions accepted in [8].

the theoretical estimates for these coefficients and compare them with known numbers [8], which follow from independent theoretical processing of experimental data. The results are collected in six Tables below. Note that in [8] somewhat different definitions of low-energy coefficients are used, so one needs to perform certain rescaling to compare the results. This is already done in the Tables I – VI.

When computing the LEC’s we have used the data [8] and [15] for the resonance parameters (listed in Appendix C); the estimated errors correspond to maximal and minimal values of the quantity under consideration. In order to save space we use the following shortened form of number recording:  $X^n \equiv X \times 10^n$ .

In the first two lines of Tables II ÷ IV and VI (three lines in Tables I and V) we also show the most significant individual contributions — those coming from  $\Delta(1232)$  and  $N(1440)$  (and from the scalar  $\sigma$  meson in the Tables I and V). The line *Full set* shows the results of summing over contributions from all the resonances listed in Appendix C. The results of independent theoretical analysis of experimental data (the lines *Data* in Tables III – VI) are taken from [8]. The lines *Data* are absent in Tables I, II because the corresponding numbers are not available in [8]. It should be kept in mind that the errors shown in the lines *Data* are just indicative. The reason is that the corresponding numbers strongly depend upon various theoretical suggestions (like, say, the value of  $S$ -wave pion-pion scattering length with isospin  $I = 0$ ; see [8]) used as the theoretical input in the process of data analysis. Clearly, it would make no sense to show the error bars in the lines which correspond to  $\sigma$ -meson contributions (Tables I and V).

As clearly seen from these Tables, only two lightest baryon resonances —  $\Delta(1232)$  and  $N(1440)$  — provide significant contributions to all the coefficients except  $a_{0j}^+$  and  $c_{0j}^+$ . From (37), (38) and (40) it follows that the meson resonances only contribute to  $\alpha(t)$ , the Table I (as well as V) shows that the values of  $a_{00}^+ \div a_{02}^+$  ( $c_{00}^+ \div c_{02}^+$ ) cannot be explained if we neglect the contribution due to famous light scalar  $\sigma$ -meson<sup>9</sup> with the mass parameter  $M_\sigma \sim 550 \div 700$  MeV and “effective coupling” (see [8])

$$G_1^0 \equiv g_{S\pi\pi} g_{NNS}^{(1)} \sim 50 \div 100 .$$

Altogether, these results show that the extended perturbation scheme provides reasonable values for the low energy coefficients already at tree level. We emphasize that this is closely

---

<sup>9</sup> This statement remains true with respect to  $a_{03}^+$  ( $c_{03}^+$ ).

Resonance	$a_{00}^+$	$a_{01}^+$	$a_{02}^+$	$a_{10}^+$	$a_{11}^+$	$a_{12}^+$	$a_{20}^+$	$a_{21}^+$	$a_{22}^+$
$\sigma(650)$	+19	+0.94	$+5.20^{-2}$						
$\Delta(1232)$	+2.74 $\pm 4.6^{-2}$	$+7.19^{-1}$ $\pm 1.2^{-2}$	$-1.66^{-2}$ $\pm 2.8^{-4}$	+6.36 $\pm 1.1^{-1}$	$-1.27^{-2}$ $\pm 2.1^{-4}$	$-4.22^{-3}$ $\pm 7.2^{-5}$	+1.16 $\pm 2.0^{-2}$	$-3.91^{-2}$ $\pm 6.6^{-4}$	$+1.83^{-4}$ $\pm 3.1^{-6}$
$N(1440)$	-3.86 $\pm 1.6$	$+4.50^{-2}$ $\pm 1.9^{-2}$	$-3.76^{-4}$ $\pm 1.6^{-4}$	$-2.71^{-1}$ $\pm 1.1^{-1}$	$+6.79^{-3}$ $\pm 2.9^{-3}$	$-1.13^{-4}$ $\pm 4.8^{-6}$	$-1.36^{-2}$ $\pm 5.7^{-3}$	$+5.69^{-4}$ $\pm 2.4^{-4}$	$-1.43^{-5}$ $\pm 6.0^{-6}$
Full set	+23.1 $\pm 6.6$	+1.63 $\pm 1.2^{-1}$	$+3.50^{-2}$ $\pm 1.7^{-3}$	+6.03 $\pm 4.4^{-1}$	$-1.02^{-2}$ $\pm 8.9^{-3}$	$-4.23^{-3}$ $\pm 1.9^{-4}$	+1.14 $\pm 2.9^{-2}$	$-3.86^{-2}$ $\pm 9.7^{-4}$	$+1.73^{-4}$ $\pm 1.0^{-5}$

TABLE I: Tree level low energy coefficients  $a_{mn}^+$  ( $m, n = 0, 1, 2$ ).

Resonance	$a_{00}^-$	$a_{01}^-$	$a_{02}^-$	$a_{10}^-$	$a_{11}^-$	$a_{12}^-$	$a_{20}^-$	$a_{21}^-$	$a_{22}^-$
$\Delta(1232)$	-7.46 $\pm 1.3^{-1}$	$-1.04^{-1}$ $\pm 1.6^{-3}$	$+5.18^{-3}$ $\pm 8.8^{-5}$	-1.36 $\pm 2.3^{-2}$	$+2.43^{-2}$ $\pm 4.1^{-4}$	$+5.14^{-4}$ $\pm 8.7^{-6}$	$-2.47^{-1}$ $\pm 4.2^{-3}$	$+1.22^{-2}$ $\pm 2.1^{-4}$	$-2.33^{-4}$ $\pm 4.0^{-6}$
$N(1440)$	-1.21 $\pm 5.1^{-1}$	$+2.02^{-2}$ $\pm 8.5^{-3}$	$-2.53^{-4}$ $\pm 1.1^{-4}$	$-6.01^{-2}$ $\pm 2.6^{-2}$	$+2.03^{-3}$ $\pm 8.5^{-4}$	$-4.24^{-5}$ $\pm 1.8^{-5}$	$-3.05^{-3}$ $\pm 1.3^{-3}$	$+1.53^{-4}$ $\pm 6.4^{-5}$	$-4.48^{-6}$ $\pm 1.9^{-6}$
Full set	-10.5 $\pm 2.0$	$-1.80^{-1}$ $\pm 6.4^{-2}$	$+4.24^{-3}$ $\pm 8.6^{-4}$	-1.45 $\pm 6.8^{-2}$	$+2.53^{-2}$ $\pm 1.7^{-3}$	$+4.86^{-4}$ $\pm 3.3^{-5}$	$-2.51^{-1}$ $\pm 5.9^{-3}$	$+1.24^{-2}$ $\pm 2.8^{-4}$	$-2.38^{-4}$ $\pm 6.1^{-6}$

TABLE II: Tree level low energy coefficients  $a_{mn}^-$  ( $m, n = 0, 1, 2$ ).

connected with the postulated Regge asymptotic conditions in the hyperlayer  $B_t$ . One can check that, once these conditions are violated, results start to differ drastically (by several orders!) from those shown in Tables I – VI. Besides, it turns out that the presence of the light scalar meson is also essential. Although the scalar mesons do not contribute to the second kind bootstrap conditions, the necessity of introducing the corresponding auxiliary fields follows from the data on  $c_{0j}^+$  ( $a_{0j}^+$ ). The simplest way to explain the values of those coefficients is to suggest the existence of at least one light scalar meson with above-specified parameters. It is interesting to note that the similar situation has revealed itself in the case of pion-kaon elastic scattering (see [5]).

Resonance	$b_{00}^+$	$b_{01}^+$	$b_{02}^+$	$b_{10}^+$	$b_{11}^+$	$b_{12}^+$	$b_{20}^+$	$b_{21}^+$	$b_{22}^+$
$\Delta(1232)$	$-5.20$ $\pm 8.8^{-2}$	$+2.09^{-1}$ $\pm 3.5^{-3}$	$-5.34^{-3}$ $\pm 9.0^{-5}$	$-9.45^{-1}$ $\pm 1.6^{-2}$	$+6.81^{-2}$ $\pm 1.2^{-3}$	$-2.90^{-3}$ $\pm 4.9^{-5}$	$-1.72^{-1}$ $\pm 2.9^{-3}$	$+1.79^{-2}$ $\pm 3.0^{-4}$	$-1.05^{-3}$ $\pm 1.8^{-5}$
$N(1440)$	$+3.37^{-1}$ $\pm 1.4^{-1}$	$-5.64^{-3}$ $\pm 2.4^{-3}$	$+7.07^{-5}$ $\pm 3.0^{-5}$	$+1.70^{-2}$ $\pm 7.1^{-3}$	$-5.67^{-4}$ $\pm 2.4^{-4}$	$+1.19^{-5}$ $\pm 5.0^{-6}$	$+8.53^{-4}$ $\pm 3.6^{-4}$	$-4.28^{-5}$ $\pm 1.8^{-5}$	$+1.25^{-6}$ $\pm 5.3^{-7}$
Full set	$-4.64$ $\pm 4.3^{-1}$	$+2.19^{-1}$ $\pm 1.2^{-2}$	$-5.25^{-3}$ $\pm 1.9^{-4}$	$-9.22^{-1}$ $\pm 2.7^{-2}$	$+6.78^{-2}$ $\pm 1.5^{-3}$	$-2.89^{-3}$ $\pm 5.6^{-5}$	$-1.71^{-1}$ $\pm 3.3^{-3}$	$+1.78^{-2}$ $\pm 3.2^{-4}$	$-1.05^{-3}$ $\pm 1.8^{-5}$
Data	$-3.50$ $\pm 1.1^{-1}$	$+2.50^{-1}$ $\pm 1.1^{-1}$	$-1.00^{-2}$ $\pm 5.0^{-3}$	$+9.6^{-2}$ $\pm 2.0^{-2}$	$+4.80^{-2}$ $\pm 4.7^{-2}$	$-1.00^{-2}$ $\pm 2.0^{-3}$	$-3.10^{-1}$ $\pm 5.0^{-2}$	$+4.80^{-2}$ $\pm 4.7^{-2}$	$-9.00^{-3}$ $\pm 3.0^{-3}$

TABLE III: Tree level low energy coefficients  $b_{mn}^+$  ( $m, n = 0, 1, 2$ ).

Resonance	$b_{00}^-$	$b_{01}^-$	$b_{02}^-$	$b_{10}^-$	$b_{11}^-$	$b_{12}^-$	$b_{20}^-$	$b_{21}^-$	$b_{22}^-$
$\Delta(1232)$	$+6.09$ $\pm 1.0^{-1}$	$-1.48^{-1}$ $\pm 2.5^{-3}$	$+2.36^{-3}$ $\pm 4.0^{-5}$	$+1.11$ $\pm 1.9^{-2}$	$-6.22^{-2}$ $\pm 1.1^{-3}$	$+2.13^{-3}$ $\pm 3.6^{-5}$	$+2.02^{-1}$ $\pm 3.4^{-3}$	$-1.78^{-2}$ $\pm 3.0^{-4}$	$+9.00^{-4}$ $\pm 1.5^{-5}$
$N(1440)$	$+1.50$ $\pm 6.3^{-1}$	$-1.26^{-2}$ $\pm 5.3^{-3}$	$+1.05^{-4}$ $\pm 4.4^{-5}$	$+7.56^{-2}$ $\pm 3.2^{-2}$	$-1.90^{-3}$ $\pm 8.0^{-4}$	$+3.17^{-5}$ $\pm 1.3^{-5}$	$+3.80^{-3}$ $\pm 1.6^{-3}$	$-1.59^{-4}$ $\pm 6.7^{-5}$	$+3.99^{-6}$ $\pm 1.7^{-6}$
Full set	$+9.55$ $\pm 2.0$	$-4.47^{-2}$ $\pm 6.0^{-2}$	$+3.60^{-3}$ $\pm 6.7^{-4}$	$+1.22$ $\pm 6.9^{-2}$	$-6.25^{-2}$ $\pm 2.4^{-3}$	$+2.15^{-3}$ $\pm 5.7^{-5}$	$+2.07^{-1}$ $\pm 5.4^{-3}$	$-1.79^{-2}$ $\pm 3.8^{-4}$	$+9.03^{-4}$ $\pm 1.7^{-5}$
Data	$+8.43$ $\pm 1.2^{-1}$	$+2.00^{-1}$ $\pm 1.2^{-1}$	$+2.00^{-2}$ $\pm 8.0^{-3}$	$+1.08$ $\pm 4.0^{-2}$	$-6.30^{-2}$ $\pm 1.2^{-2}$	$+4.00^{-3}$ $\pm 1.9^{-3}$	$+3.10^{-1}$ $\pm 4.0^{-2}$	$-3.60^{-2}$ $\pm 2.8^{-2}$	$+3.00^{-3}$ $\pm 1.0^{-3}$

TABLE IV: Tree level low energy coefficients  $b_{mn}^-$  ( $m, n = 0, 1, 2$ ).

## X. CONCLUSIONS

The numerical analysis of bootstrap constraints for the tree level amplitude of elastic pion-nucleon scattering shows that both physical (Regge-like asymptotic behavior) and mathematical (uniformity and summability principles) postulates, used as the basis for extended perturbation scheme suggested in the series of papers [1] – [5], look quite reasonable. In those cases when experimental data on the resonance spectrum allow to check the consistency of corresponding sum rules, the results are satisfactory. It is interesting to note that,

Resonance	$c_{00}^+$	$c_{01}^+$	$c_{02}^+$	$c_{10}^+$	$c_{11}^+$	$c_{12}^+$	$c_{20}^+$	$c_{21}^+$	$c_{22}^+$
$\sigma(650)$	+19	+0.94	+5.20 <sup>-2</sup>						
$\Delta(1232)$	+2.74 $\pm 4.6^{-1}$	+7.18 <sup>-1</sup> $\pm 1.2^{-2}$	-1.66 <sup>-2</sup> $\pm 2.8^{-4}$	+1.17 $\pm 9.8^{-2}$	+1.68 <sup>-1</sup> $\pm 1.4^{-3}$	-8.56 <sup>-3</sup> $\pm 4.6^{-5}$	+2.12 <sup>-1</sup> $\pm 1.8^{-2}$	+2.38 <sup>-2</sup> $\pm 6.4^{-4}$	-2.37 <sup>-3</sup> $\pm 1.5^{-5}$
$N(1440)$	-3.86 $\pm 1.6$	+4.50 <sup>-2</sup> $\pm 1.9^{-2}$	-3.76 <sup>-4</sup> $\pm 1.6^{-4}$	+6.65 <sup>-2</sup> $\pm 1.3^{-1}$	+3.02 <sup>-3</sup> $\pm 2.0^{-3}$	-6.37 <sup>-5</sup> $\pm 2.4^{-5}$	+3.35 <sup>-3</sup> $\pm 6.4^{-3}$	+9.59 <sup>-5</sup> $\pm 1.7^{-4}$	-5.04 <sup>-6</sup> $\pm 3.1^{-6}$
Full set	+23.1 $\pm 6.6$	+1.63 $\pm 1.2^{-1}$	+3.50 <sup>-2</sup> $\pm 1.7^{-3}$	+1.39 $\pm 4.3^{-1}$	+1.83 <sup>-1</sup> $\pm 7.9^{-3}$	-8.41 <sup>-3</sup> $\pm 1.2^{-4}$	+2.19 <sup>-1</sup> $\pm 2.8^{-2}$	+2.40 <sup>-2</sup> $\pm 8.6^{-4}$	-2.37 <sup>-3</sup> $\pm 1.9^{-5}$
Data	+25.6 $\pm 5.0^{-1}$	+1.18 $\pm 5.0^{-2}$	+3.55 <sup>-2</sup> $\pm 7.0^{-3}$	+1.18 $\pm 5.0^{-2}$	+1.53 <sup>-1</sup> $\pm 1.7^{-2}$	-1.50 <sup>-2</sup> $\pm 3.0^{-3}$	+2.00 <sup>-1</sup> $\pm 1.0^{-2}$	+3.40 <sup>-2</sup> $\pm 1.0^{-3}$	-8.00 <sup>-3</sup> $\pm 1.0^{-3}$

TABLE V: Tree level low energy coefficients  $c_{mn}^+$  ( $m, n = 0, 1, 2$ ).

Resonance	$c_{00}^-$	$c_{01}^-$	$c_{02}^-$	$c_{10}^-$	$c_{11}^-$	$c_{12}^-$	$c_{20}^-$	$c_{21}^-$	$c_{22}^-$
$\Delta(1232)$	-1.37 $\pm 1.1^{-1}$	-2.18 <sup>-1</sup> $\pm 1.6^{-3}$	+6.91 <sup>-3</sup> $\pm 3.6^{-5}$	-2.49 <sup>-1</sup> $\pm 2.1^{-2}$	-3.18 <sup>-2</sup> $\pm 5.2^{-4}$	+2.33 <sup>-3</sup> $\pm 1.3^{-5}$	-4.52 <sup>-2</sup> $\pm 3.8^{-3}$	-4.35 <sup>-3</sup> $\pm 1.8^{-4}$	+5.74 <sup>-4</sup> $\pm 5.2^{-6}$
$N(1440)$	+2.97 <sup>-1</sup> $\pm 5.7^{-1}$	+1.59 <sup>-2</sup> $\pm 5.8^{-3}$	-1.71 <sup>-4</sup> $\pm 5.0^{-5}$	+1.49 <sup>-2</sup> $\pm 2.9^{-2}$	+5.52 <sup>-4</sup> $\pm 6.1^{-4}$	-1.89 <sup>-5</sup> $\pm 9.2^{-6}$	+7.51 <sup>-4</sup> $\pm 1.4^{-3}$	+1.52 <sup>-5</sup> $\pm 4.7^{-5}$	-1.26 <sup>-6</sup> $\pm 1.0^{-7}$
Full set	-1.00 $\pm 2.0$	-1.77 <sup>-1</sup> $\pm 4.4^{-2}$	+7.80 <sup>-3</sup> $\pm 4.7^{-4}$	-2.27 <sup>-1</sup> $\pm 6.8^{-2}$	-3.05 <sup>-2</sup> $\pm 1.5^{-3}$	+2.33 <sup>-3</sup> $\pm 2.6^{-5}$	-4.43 <sup>-2</sup> $\pm 5.6^{-3}$	-4.31 <sup>-3</sup> $\pm 2.3^{-4}$	+5.72 <sup>-4</sup> $\pm 6.4^{-6}$
Data	-5.05 <sup>-1</sup> $\pm 4.5^{-2}$	-9.70 <sup>-2</sup> $\pm 1.2^{-2}$	+9.00 <sup>-3</sup> $\pm 7.0^{-3}$	-1.63 <sup>-1</sup> $\pm 7.0^{-3}$	-3.90 <sup>-2</sup> $\pm 5.0^{-3}$	-5.00 <sup>-3</sup> $\pm 2.0^{-3}$	-3.80 <sup>-2</sup> $\pm 4.0^{-3}$	-1.30 <sup>-2</sup> $\pm 4.0^{-3}$	+3.00 <sup>-3</sup> $\pm 1.0^{-3}$

TABLE VI: Tree level low energy coefficients  $c_{mn}^-$  ( $m, n = 0, 1, 2$ ).

in general, these sum rules possess certain features of supersymmetry since they connect among themselves the parameters of meson and baryon spectra. Besides, numerical tests show that our sum rules confirm the so-called local cancellation hypotheses suggested in the series of papers [16].

Moreover, as follows from the results of Sec. IX, already the first term (trees) of the extended Dyson series provides reasonable numerical values for the low energy coefficients



which certainly acquire contributions from the higher order terms. This gives us a hope that the latter terms will result just in small corrections. If so, this would mean that the general philosophy of quasiparticle method (see [17]) can be successfully applied to the case of effective scattering theory of strong interaction.

In subsequent publication we will show that these conclusions hold also for elastic kaon-nucleon scattering.

### Acknowledgements

We are grateful to V. A. Franke, H. Nielsen, P. Osland, S. Paston, J. Schechter, A. Tochin, A. Vasiliev and M. Vyazovski for stimulating discussions. The work was supported in part by INTAS (project 587, 2000) and by the Russian National Programme (grant RNP 2.1.1.1112). The work by A. Vereshagin was supported by L. Meltzers Høyskolefond (Studentprosjektstipend, 2004).

## APPENDIX A: CONTRACTED PROJECTING OPERATORS

In practical calculations in the framework of the effective scattering theory approach one never needs to use the explicit form of spin sums. It turns out sufficient to exploit the formalism of so-called *contracted projecting operators* based on the properties of Rarita-Schwinger wave functions. Although this formalism has been developed nearly forty years ago in the series of papers [10] (see also [11], [12], [13] and references therein), it is still not widely known. That is why in this Appendix we present a short summary of corresponding formulae.

Let us first consider the case of a free boson field with the mass parameter  $M$ , momentum  $p_\mu$  ( $p^2 = M^2$ ), spin  $J = l = 1, 2, \dots$  and polarization  $i = -l, \dots, l$ . The corresponding wave function is described by a symmetric traceless tensor  $\mathcal{E}_{\mu_1 \dots \mu_l}(i, p)$  which satisfies the following

conditions:

$$\mathcal{E}_{\dots\mu_m\dots\mu_n\dots}(i, p) = \mathcal{E}_{\dots\mu_n\dots\mu_m\dots}(i, p) \quad (\text{symmetry}),$$

$$g^{\mu_m\mu_n}\mathcal{E}_{\dots\mu_m\dots\mu_n\dots}(i, p) = 0 \quad (\text{tracelessness}),$$

$$p^{\mu_m}\mathcal{E}_{\dots\mu_m\dots}(i, p) = 0 \quad (\text{transversality}),$$

$$[\mathcal{E}_{\mu_1\dots\mu_l}(i, p)]^* \mathcal{E}^{\mu_1\dots\mu_l}(j, p) = (-1)^l \delta_{ij} \quad (\text{normalization}).$$

The *spin sum* is defined as follows (for  $p^2 = M^2$ )

$$\Pi_{\nu_1\dots\nu_l}^{\mu_1\dots\mu_l}(p; l) \equiv \sum_{i=-l}^l \mathcal{E}^{\mu_1\dots\mu_l}(i, p) [\mathcal{E}_{\nu_1\dots\nu_l}(i, p)]^* . \quad (\text{A1})$$

Typically, when computing a given  $S$ -matrix element one only needs to know the so-called *contracted projector*

$$\mathcal{P}^{(l)}(k, k', p) \equiv k^{\nu_1} \dots k^{\nu_l} \Pi_{\nu_1\dots\nu_l}^{\mu_1\dots\mu_l}(p; l) k'_{\mu_1} \dots k'_{\mu_l} , \quad (\text{A2})$$

where  $k$  and  $k'$  stand for arbitrary 4-momenta. The inverse relation

$$\Pi_{\nu_1\dots\nu_l}^{\mu_1\dots\mu_l}(p; l) = \frac{1}{(l!)^2} \frac{\partial}{\partial k^{\nu_1}} \dots \frac{\partial}{\partial k^{\nu_l}} \frac{\partial}{\partial k'_{\mu_1}} \dots \frac{\partial}{\partial k'_{\mu_l}} \mathcal{P}^{(l)}(k, k', p) \quad (\text{A3})$$

gives the form of spin sum (A1) when the explicit expression for contracted projector (A2) is known<sup>10</sup>. As shown in the above-cited articles, this expression reads

$$\mathcal{P}^{(l)}(k, k', p) = \frac{(-1)^l l!}{(2l-1)!!} |\hat{k}|^l |\hat{k}'|^l P_l \left( \frac{(\hat{k}\hat{k}')}{|\hat{k}||\hat{k}'|} \right) . \quad (\text{A4})$$

Here the following compact notations are used:

$$\begin{aligned} \hat{k}_\mu &\equiv k_\mu - \frac{(pk)}{M^2} p_\mu ; & \hat{k}'_\mu &\equiv k'_\mu - \frac{(pk')}{M^2} p_\mu ; \\ |\hat{r}| &\equiv \sqrt{[(\hat{r}\hat{r})]} , (r = k, k'). \end{aligned} \quad (\text{A5})$$

---

<sup>10</sup> In the case under consideration we only need to know the form of the contracted projector with two external momenta ( $k_\mu$  and  $k'_\mu$ ).

Let us now consider the case of a fermion with spin  $J = l + 1/2$  ( $l = 0, 1, \dots$ ), mass parameter  $M$  and polarization  $j = -(l + \frac{1}{2}), \dots, +(l + \frac{1}{2})$ . Two corresponding wave functions (particle and anti-particle) are defined as symmetric traceless spin-tensors<sup>11</sup>  $\mathcal{U}_{\rho\mu_1\dots\mu_l}^\pm(j, p)$  and  $\bar{\mathcal{U}}_{\rho\mu_1\dots\mu_l}^\pm(j, p) \equiv (\mathcal{U}^\mp)^\dagger \gamma_0$ . Here the vector indices  $\mu_1 \dots \mu_l = 0, 1, 2, 3$ , while the spinor one  $\rho = 1, 2, 3, 4$ . The set of auxiliary conditions (at  $p^2 = M^2$ ) reads:

$$\mathcal{U}_{\rho\dots\mu_m\dots\mu_n\dots}^\pm(j, p) = \mathcal{U}_{\rho\dots\mu_n\dots\mu_m\dots}^\pm(j, p) \quad (\text{symmetry}),$$

$$g^{\mu_m\mu_n}\mathcal{U}_{\rho\dots\mu_m\dots\mu_n\dots}^\pm(j, p) = 0 \quad (\text{tracelessness}),$$

$$p^{\mu_m}\mathcal{U}_{\rho\dots\mu_m\dots}^\pm(j, p) = 0 \quad (p\text{-transversality}),$$

$$(\gamma^{\mu_m})_{\rho\tau}\mathcal{U}_{\tau\dots\mu_m\dots}^\pm(j, p) = 0 \quad (\gamma\text{-transversality}),$$

$$\sum_{\rho;\mu_1\dots\mu_l} \bar{\mathcal{U}}_{\rho\mu_1\dots\mu_l}^+(i, p)\mathcal{U}_{\rho}^{-\mu_1\dots\mu_l}(j, p) = (-1)^l 2M\delta_{ij} \quad (\text{normalization}),$$

$$\begin{aligned} (\not{p} \pm M)_{\rho\tau}\mathcal{U}_{\tau\mu_1\dots\mu_l}^\pm(j, p) &= 0, \\ \bar{\mathcal{U}}_{\rho\mu_1\dots\mu_l}^\pm(j, p)(\not{p} \mp M)_{\rho\tau} &= 0 \quad (\text{wave equations}). \end{aligned}$$

In this case the spin sum

$$\begin{aligned} \Pi_{\nu_1\dots\nu_l}^{\mu_1\dots\mu_l}{}_{\rho\tau}(p; l + 1/2) &\equiv \\ \sum_{j=-(l+1/2)}^{j=+(l+1/2)} \mathcal{U}_{\rho\nu_1\dots\nu_l}^-(j, p)\bar{\mathcal{U}}_{\tau}^{+\mu_1\dots\mu_l}(j, p) \end{aligned} \quad (\text{A6})$$

as well as the corresponding contracted projector

$$\begin{aligned} \mathcal{P}_{\rho\tau}^{(l+\frac{1}{2})}(k, k', p) &\equiv \\ k^{\nu_1} \dots k^{\nu_l} \Pi_{\nu_1\dots\nu_l}^{\mu_1\dots\mu_l}{}_{\rho\tau}(p; l + 1/2) k'^{\mu_1} \dots k'^{\mu_l} \end{aligned} \quad (\text{A7})$$

---

<sup>11</sup> To save space in this Appendix we use the spinor notations accepted in [18]. The correspondence with conventionally used notations (see, e.g., [19]) is provided by the relations:  $\mathcal{U}^+ \equiv v$ ,  $\mathcal{U}^- \equiv u$ ,  $\bar{\mathcal{U}}^+ \equiv \bar{u}$ ,  $\bar{\mathcal{U}}^- \equiv \bar{v}$ .

are  $4 \times 4$  matrices in spinor space (in what follows we omit spinor indices). The relation analogous to (A4) reads

$$\mathcal{P}^{(l+\frac{1}{2})}(k, k', p) = \frac{(-1)^l l!}{(2l+1)!!} |\hat{k}|^l |\hat{k}'|^l \left\{ P'_{l+1} \left( \frac{\hat{k}_\mu \hat{k}'^\mu}{|\hat{k}| |\hat{k}'|} \right) - \frac{\hat{k} \hat{k}'}{|\hat{k}| |\hat{k}'|} P'_l \left( \frac{\hat{k}_\mu \hat{k}'^\mu}{|\hat{k}| |\hat{k}'|} \right) \right\} (p+M), \quad (\text{A8})$$

where  $P_l(\chi)$  is the Legendre polynomial and  $P'_l(\chi)$  is its derivative with respect to  $\chi$ . Note that at  $p^2 = M^2$  the matrices  $\hat{k} \hat{k}'$  and  $\not{p}$  commute with one another, so the position of the term  $(p+M)$  does not matter as long as one only needs to know the numerator of minimal propagator.

## APPENDIX B: RESONANCE EXCHANGE CONTRIBUTIONS

Below we give the full list of contributions to invariant amplitudes  $A^\pm$  and  $B^\pm$  provided by the resultant graphs with  $s$ - and  $t$ -channel exchanges (see Fig. 1). The contributions of the graphs with  $u$ -channel resonances can be obtained from those with  $s$ -channel ones with the help of corresponding substitution.

We employ the notations of Sec. III; the auxiliary functions  $\Phi(M, m, \mu)$ ,  $F_A^l(M, \chi)$  and  $F_B^l(M, \chi)$  are defined in (19) — (21). As always throughout the paper,  $m$  and  $\mu$  are the nucleon and pion masses,  $M$  is the resonance mass,  $P_l(\chi)$  is the Legendre polynomial and  $P'_l(\chi)$  — its derivative with respect to argument. Introducing the abbreviation  $(\not{k} + \not{k}')/2 \equiv \mathcal{Q}$  and compact notation for baryon numerical factors:

$$G(\pi NB) = |g_B(J, I, \mathcal{N}_B)|^2 (\Phi)^l \frac{l!}{(2l+1)!!}, \quad (\text{B1})$$

where  $B$  refers to any relevant baryon of spin  $J = l + 1/2$ , isospin  $I$  and normality  $\mathcal{N}_B$ , we get the following expressions for the  $x$ -channel ( $x = s, u$ ) baryon exchange graphs (see Fig. 7 **a, b**):

$$T_{\beta\alpha, ba}^I(Z_x) \bar{u}(p', \lambda') \left\{ -\frac{G(\pi NB)}{x - M_R^2} [F_A^l(-\mathcal{N}_B M, t) + Z_x \mathcal{Q} F_B^l(-\mathcal{N}_B M, t)] \right\} u(p, \lambda). \quad (\text{B2})$$

Here

$$Z_s = 1, \quad Z_u = -1,$$

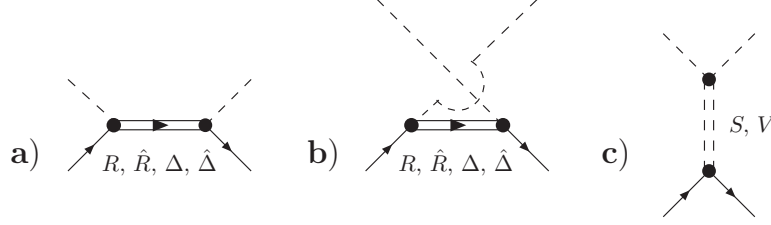


FIG. 7: Resonance exchange graphs: **a**:  $I = 1/2, 3/2$  in  $s$ -channel; **b**:  $I = 1/2, 3/2$  in  $u$ -channel; **c**:  $I = 0, 1$  in  $t$ -channel;

and

$$T_{\beta\alpha,ba}^{1/2}(Z_x) \equiv (\delta_{ba}\delta_{\beta\alpha} + Z_x i\varepsilon_{bac}(\sigma_c)_{\beta\alpha});$$

$$T_{\beta\alpha,ba}^{3/2}(Z_x) \equiv \left( -\frac{2}{3}\delta_{ba}\delta_{\beta\alpha} + Z_x \frac{i}{3}\varepsilon_{bac}(\sigma_c)_{\beta\alpha} \right).$$

Further, using

$$F(M, m, \mu) \equiv \frac{1}{4} \sqrt{|(M^2 - 4m^2)(M^2 - 4\mu^2)|} \quad (\text{B3})$$

and the compact notation for meson numerical factors ( $I = S, V$  stands for isoscalar and isovector, respectively; the constants  $g_{I\pi\pi}$  and  $g_{NNI}^{(n)}$  are introduced in (8) – (11))

$$G_n^I \equiv (F)^J g_{I\pi\pi} g_{NNI}^{(n)} \frac{J!}{(2J-1)!!}, \quad (n = 1, 2), \quad (\text{B4})$$

we obtain the contributions due to the meson exchange graphs (see Fig. 7 c):

$$T_{ba,\beta\alpha}^I \bar{u}(p', \lambda') \mathcal{M}^I u(p, \lambda),$$

where

$$T_{ba,\beta\alpha}^S \equiv -\delta_{ba} \delta_{\beta\alpha}, \quad T_{ba,\beta\alpha}^V \equiv i\varepsilon_{bac}(\sigma_c)_{\beta\alpha},$$

and

$$\mathcal{M}^I \equiv \frac{G_1^I}{t - M_I^2} P_J \left( \frac{s-u}{4F} \right) + \frac{G_2^I}{t - M_I^2} \left\{ \frac{4m}{M_I^2 - 4m^2} P'_{J-1} \left( \frac{s-u}{4F} \right) + \mathcal{Q} \frac{1}{F} P'_J \left( \frac{s-u}{4F} \right) \right\}$$

(it is assumed that  $P'_{-1}(\chi) \equiv 0$ ). Note that in this expression  $t$  and  $s-u \equiv \nu_t$  are independent variables; the residue at  $t = M^2$  may (and does) depend on  $\nu_t$ .

## APPENDIX C: LIST OF BARYON RESONANCES

In Table VII we give a list of  $N$  and  $\Delta$  baryon resonances which we take into account when testing our sum rules. Here  $J$ ,  $I$ ,  $P$  and  $\mathcal{N}$  stand for the resonance spin, isospin, parity and normality, respectively. The minimal and maximal values of  $G(\pi NR)$  have been calculated using the data from [15].

$R$	$I$	$J$	$P(\mathcal{N})$	$G(\pi NR)$
$N(940)$	$1/2$	$1/2$	$+(+)$	$179.7$
$N(1440)$	$1/2$	$1/2$	$+(+)$	$26.0 \div 63.9$
$N(1680)$	$1/2$	$5/2$	$+(+)$	$6.06 \div 7.60$
$N(1710)$	$1/2$	$1/2$	$+(+)$	$0.36 \div 3.6$
$N(1720)$	$1/2$	$3/2$	$+(-)$	$0.09 \div 0.35$
$N(2220)$	$1/2$	$9/2$	$+(+)$	$0.94 \div 2.7$
$N(1520)$	$1/2$	$3/2$	$-(+)$	$7.35 \div 10.9$
$N(1535)$	$1/2$	$1/2$	$-(-)$	$0.30 \div 0.67$
$N(1650)$	$1/2$	$1/2$	$-(-)$	$0.54 \div 1.09$
$N(1675)$	$1/2$	$5/2$	$-(-)$	$0.28 \div 0.45$
$N(1700)$	$1/2$	$3/2$	$-(+)$	$0.19 \div 1.68$
$N(2190)$	$1/2$	$7/2$	$-(+)$	$0.9 \div 4.3$
$N(2250)$	$1/2$	$9/2$	$-(-)$	$0.05 \div 0.53$
$N(2600)$	$1/2$	$11/2$	$-(+)$	$0.43 \div 1.40$
$R$	$I$	$J$	$P(\mathcal{N})$	$G(\pi NR)$
$\Delta(1232)$	$3/2$	$3/2$	$+(-)$	$4.17 \div 4.31$
$\Delta(1600)$	$3/2$	$3/2$	$+(-)$	$0.49 \pm 2.2$
$\Delta(1905)$	$3/2$	$5/2$	$+(+)$	$3.5 \div 8.7$
$\Delta(1910)$	$3/2$	$1/2$	$+(+)$	$4.8 \div 9.7$
$\Delta(1920)$	$3/2$	$3/2$	$+(-)$	$0.12 \div 0.94$
$\Delta(1950)$	$3/2$	$7/2$	$+(-)$	$1.29 \div 3.36$
$\Delta(2420)$	$3/2$	$11/2$	$+(-)$	$0.19 \div 0.97$
$\Delta(1620)$	$3/2$	$1/2$	$-(-)$	$0.51 \div 0.86$
$\Delta(1700)$	$3/2$	$3/2$	$-(+)$	$4.5 \div 17.9$
$\Delta(1930)$	$3/2$	$5/2$	$-(-)$	$0.19 \div 1.04$
$\Delta(1950)$	$3/2$	$7/2$	$+(-)$	$1.3 \div 2.4$
$\Delta(2420)$	$3/2$	$11/2$	$+(-)$	$0.2 \div 1.0$

TABLE VII:  $N$  and  $\Delta$ -baryon summary table.

- 
- [1] A. Vereshagin and V. Vereshagin, Phys. Rev. D **69**, 025002 (2004).
  - [2] K. Semenov-Tian-Shansky, A. Vereshagin, and V. Vereshagin, Phys. Rev. D **73**, 025020 (2006).
  - [3] A. Vereshagin, V. Vereshagin, and K. Semenov-Tian-Shansky, J. Math. Sci. **125**, 144 (2005).  
This article originally appeared in Zap. Nauchn. Sem. POMI **291**, 78 (2002) (in Russian).
  - [4] V. Vereshagin, Phys. Rev. D **55**, 5349 (1997).
  - [5] A. Vereshagin and V. Vereshagin, Phys. Rev. D **59**, 016002 (1998).
  - [6] A. Vereshagin and V. Vereshagin,  $\pi N$  Newsletter **15**, 288 (1999); A. Vereshagin,  $\pi N$  Newsletter **16**, 426 (2002).
  - [7] K. Semenov-Tian-Shansky, A. Vereshagin, and V. Vereshagin, *Tenth International Conference on Hadron Spectroscopy, Aschaffenburg, Germany, 2003*, edited by E.Klempt, H.Koch, and H.Orth, AIP Conf. Proc. No. 717 (AIP, New York, 2004).  
Three talks given by V. Vereshagin, K. Semenov-Tian-Shansky, and A. Vereshagin at HSQCD04, Proceedings of the First International Workshop “*Hadron Structure and QCD: from LOW to HIGH energies*”, Repino, St. Petersburg, Russia, 2004, edited by V. T. Kim and L. N. Lipatov (PNPI, Gatchina, St. Petersburg, 2004); pp. 285, 291, 297.  
A. Vereshagin, in *XVIIIth International Workshop “High Energy Physics and Quantum Field Theory”*, St.Petersburg, Peterhof, Russia, 2004, edited by M. Dubinin and V. Savrin, QFTHEP’2004 International Workshop Proc. (MSU, Moscow, 2005), p. 291.
  - [8] M. M. Nagels *et al.*, Nucl. Phys. **B109**, 1 (1976); *ibid* **B147**, 189 (1979); O. Dumbrajs *et al.*, Nucl. Phys. **B216** 277 (1983).
  - [9] W. Rarita and J. Schwinger, Phys. Rev. **60**, 61 (1941).
  - [10] S. Weinberg, Phys. Rev. **133**, B1318 (1964); *ibid* **134**, B882 (1964); *ibid* **135**, B1049 (1964); *ibid* **138**, B988 (1965); *ibid* **181**, 1893 (1969).
  - [11] S. Weinberg, *The Quantum Theory of Fields*, vols. 1–3 (Cambridge University Press, Cambridge, England, 2000).
  - [12] V. de Alfaro, S. Fubini, G. Furlan, C. Rossetti, *Currents in Hadron Physics* (North-Holland, Amsterdam, 1973).
  - [13] M. D. Scadron, Phys. Rev. **165**, 1640 (1968).
  - [14] P. D. B. Collins, *An Introduction to Regge Theory and High-Energy Physics* (Cambridge



- University Press, Cambridge, England, 1977).
- [15] Particle Data Group, *Review of Particle Physics*, J. Phys. G: Nucl. Part. Phys. **33**, 1 (2006).
  - [16] M. Harada, F. Sannino, J. Schechter, Phys. Rev. D **54**, 1991 (1996); D. Black, A. Fariborz, F. Sannino, and J. Schechter, Phys. Rev. D **58**, 054012 (1998); *ibid*, D **59**, 074026 (1999); see also D. Black, A. Fariborz, S. Moussa, S. Nasri, and J. Schechter, Phys. Rev. D **64**, 014031 (2001).
  - [17] S. Weinberg, Phys. Rev. **130**, 776 (1963); *ibid* **131**, 440 (1963); *ibid* **133**, B232 (1964); M. Scadron and S. Weinberg, Phys. Rev. **133**, B1589 (1964); M. Scadron, S. Weinberg and J. Wright, Phys. Rev. **135**, B202 (1964).
  - [18] N. N. Bogoliubov and D. V. Shirkov, *Introduction to the Theory of Quantized Fields* (Wiley-Interscience, New York, 1980).
  - [19] M. E. Peskin and D. V. Schroeder, *An Introduction to Quantum Field Theory* (Addison-Wesley, New York, 1997).